Unraveling the Temperature and Density Structure of W 3 IRS 5

Christiaan Boersma June 2002 - March 2003

Kapteyn Institute Rijks*universiteit* Groningen
Landleven 12
9700 AV Groningen

Supervisors: dr. Frank Helmich (SRON) & dr. Russ Shipman (SRON)

Abstract

As part of their third year study in astronomy, students at the Rijks*universiteit* Groningen (R*u*G) do a 'klein onderzoek'. One of the goals of the 'klein onderzoek' is the preparation for the 'groot onderzoek', which is a graduation research project. This is the 'klein onderzoek' report on *Unraveling the Temperature and Density Structure of W 3 IRS 5*.

The topic of this 'klein onderzoek' is finding the density and temperature structure of high-mass star-forming regions. The aim of the research is to develop and standardize the method for the determination of these parameters. The test-case and Benchmark for the method is IRS 5, a bright mid-infrared source located at approximately 2.3 kpc in the GMC (Giant Molecular Cloud) W 3.
The research is focused on reproducing the SED (Spectral Energy Distribution) from Campbell et al. (1995) of IRS 5. Determination of the temperature and density structure is done by the computer program CSDUST3 from Egan et al. (1988). CSDUST3 is the implementation of the model for radiative transfer in DIDC (Dense Interstellar Dust Clouds) from Leung (1975, 1976b). The data needed for the SED are also taken from CSDUST3.
Since CSDUST3 uses quite extensive and 'unreadable' input and output files, an user interface program, BuI (Boersma user Interface) has been written to overcome this. BuI is also able to create direct graphical representations of some parameters. Standardizing the method for the determination of the density and temperature structure has become answering the question which input parameters to give to CSDUST3.

A quite extensive overview is given on how to determinate the input parameters. The agreement with the results from Campbell et al. (1995) are not 100% which is thought to be mainly the cause from the use of a somewhat different dust model. Draine & Li was used instead of Draine & Lee (1984) used by Campbell et al. (1995). An other cause could be that Campbell et al. (1995) handle the data at the same wavelength, but with different beams, different then was done here.

As an extra test the mass of IRS 5 and the temperature at the outer boundary has been estimated. The results were compared with those found by van der Tak et al. (2000). For the mass 825 $M_\odot$ was found and for the temperature at the outer boundary 35 K was found. Both compare well with the results found by van der Tak et al. (2000). Overall it can be stated that the developed method is successful and complete.

Contents

Introduction

The topic of this research is finding the density and temperature structure of high mass-star-forming regions. The aim of the research is to develop and standardize the method for the determining of these parameters. The object IRS 5 located in the Giant Molecular Cloud (GMC) W 3 will be used as the test-case and Benchmark.

The formation of high-mass stars occurs in the dense cores of GMCs. There, O and B stars, together with low mass stars form new stellar clusters. In current scenarios for star-formation there are still a lot of details lacking. This is mainly due to three reasons:

- Large dust column densities make the cores of GMCs very opaque. Practically no visual light can reach us and most of the infrared light is absorbed and/or scattered.
- Many processes such as gravitational contraction, outflow activity, transport of material in disks (if present) and chemistry all have very short and approximately the same timescale. This makes modeling very difficult because all processes have to be included and treated simultaneously for a complete and correct description.
- Distances are large. The well-known, nearest region of star-formation, Orion, is already at 400 parsecs, others are even at much larger distances. The large distances make resolution a serious problem.

Keeping this in mind, however it is not impossible to study these cores in which high-mass star-formation occurs. What is needed is the total picture of the density distribution, the temperature distribution, the molecular abundance and the chemistry. The contribution of this research to the study is the standardization of the determination of the density and temperature distribution.

Determination of the density and the temperature distribution ($n(r)$, $T(r)$) is based on the model on radiative transport in DIDC (Dense Interstellar Dust Clouds) from Leung (1975, 1976b). The model incorporates radiative transport, a dust model, a modeled interstellar radiation field, an internal radiation field, a spatial- and wavelength grid and beam convolution.

The program CSDUST3 from Egan et al. (1988) implements the model from Leung (1975) Leung (1976b) and is used here. The used dust model is that from Draine & Lee (1984). The used modeled interstellar radiation field is that (assumed) from Leung (1975, 1976b), but also the model from Mathis et al. (1983) is presented. The remaining parameters are taken from Campbell et al. (1995).

The spectral energy distribution (SED) is calculated from the results of the model and compared with the SED of IRS 5 calculated by Campbell et al. (1995). This is the main test of our approach. As additional tests the total mass and the temperature at the outer boundary of IRS 5 are estimated and compared with the results found by van der Tak et al. (2000).

The research is divided into four phases, approximately adding up to 6 months work. Phase one is literature research, phase two data gathering, phase three modeling and phase four finalization; see Table 1 for the estimated times. The planned period was June

- September (2002), but it took somewhat more time. When in September regular courses started again less time came available for the research and progress slowed down.

Phase	Description	Time
1. Literature research	Understanding radiative transport and CSDUST3	Two months
2. Data gathering	Get existing sub-mm data on W 3 IRS 5	Half a month
3. Modeling	Run various models	One-and-a-halve month
4. Finalization	Gather all data and produce final report	Two months

Table 1: The four research phases with a short description and the estimated timescales.

Some time has been invested in creating a command based user interface around CSDUST3. The program, BuI (Boersma user Interface), should make working with the excessive input and output files easier, better structured and easier visualized, since BuI is also capable to give direct graphical representation of some parameters.

This report will present its material in six parts. The first part is a description of W 3 GMC and IRS 5. The second part is a short description of the radiative transport model from Leung (1975, 1976b) and a short description on CSDUST3 from Egan et al. (1988). The third part is an overview of the gathered data and the input parameters to CSDUST3. The fourth part gives an overview of the results. The fifth part is the discussion of the results and finally, in the sixth part the summary and conclusions are presented.

1 W 3 Giant Molecular Cloud

The W 3 GMC (W is from Westerhout) is a well studied molecular cloud with several high-mass star-formation cores. W 3 has already been extensively observed. It is located in the Perseus arm at a distance of $\approx$ 2.3 kpc (Georgelin & Georgelin 1976), which makes it one of the nearest high-mass star-formation regions. The cloud consists of several dense cores, radio objects and luminous infrared objects, such as IRS 5.

1.1 W 3 The Cloud

W 3 is a radio emission source and it consists of multiple compact and ultra compact HII regions. It was first discovered by Westerhout in 1958. The soon after found water (H_2O) and hydroxyl (OH) masers show that W 3 is a very active region. After the discovery of W 3(H_2O), also known as the "Turner-Welch" object (Turner and Welch 1984), located $7''$ off W 3(OH), research shifted from the OH masers to the H_2O maser. Studies performed on the HII regions show that they represent different stages of star-formation.

W 3 has two massive and dense star-formation regions; W 3(Main) in the North and W 3(OH) in the South. The two regions are separated by $\sim 16'$. W 3(Main) has a diameter of $5'$ and is mainly ionized by associations of recently formed O/B-stars. W 3(Main) has itself two dense cores; W 3(West) and W 3(East). An overview of the region is presented

in Fig. 1. Four bright radio sources are indicated with W 3(A) through W 3(D) and there are also 8 fainter components. The brightest mid-infrared source IRS 1 has been identified with the HII region W 3(A). IRS 2 has been identified with the stars ionizing W 3(A). IRS 3 and IRS 4 respectively are associated with W 3(B) and W 3(C). Some of the overall properties of W 3 are given in Table 2.

Object	W 3
Type	Giant Molecular Cloud
Estimated Mass	7×10^4 $M_\odot$ (Lada et al. 1978)
Coordinates	RA 02 27 03.9 Dec +61 52 25 (B1950.0)
Distance	$\sim$ 2.3 kpc

Table 2: Some of the overall properties of W 3.

1.2 W 3 IRS 5

W 3 IRS 5 is a bright mid-infrared source with a faint radio counterpart located towards W 3(East). IRS 5 consists of a cluster of seven recently formed B0.5 - B0 stars with a separation of maximum 2.5″ Claussen et al. (1994). Molecular line maps of W 3 reveal a massive outflow of molecular material from IRS 5. An overview of some of the properties of W 3 are given in Table 2.

Object	W 3 IRS 5
Type	Bright mid-infrared source
Coordinates	RA 02 21 53 Dec +61 52 20 (B1950.0)
Luminosity	1.4×10^5 $L_\odot$ (Verner et al. 1980)

Table 3: Some of the Properties of W 3 IRS 5.

2 Model

Dust grains are very important for the thermodynamics of circumstellar clouds. The presence of dust grains in circumstellar clouds are indicated by infrared observations. Modeling radiative transport in circumstellar clouds containing dust can help understanding them. For realistic modeling, effects of multiple scattering, absorption and re-emission of photons must be included. Also the geometry in which the radiative transport takes place should be taken into account.

In this section the model from Leung (1975, 1976b) on radiative transport in DIDC (Dense

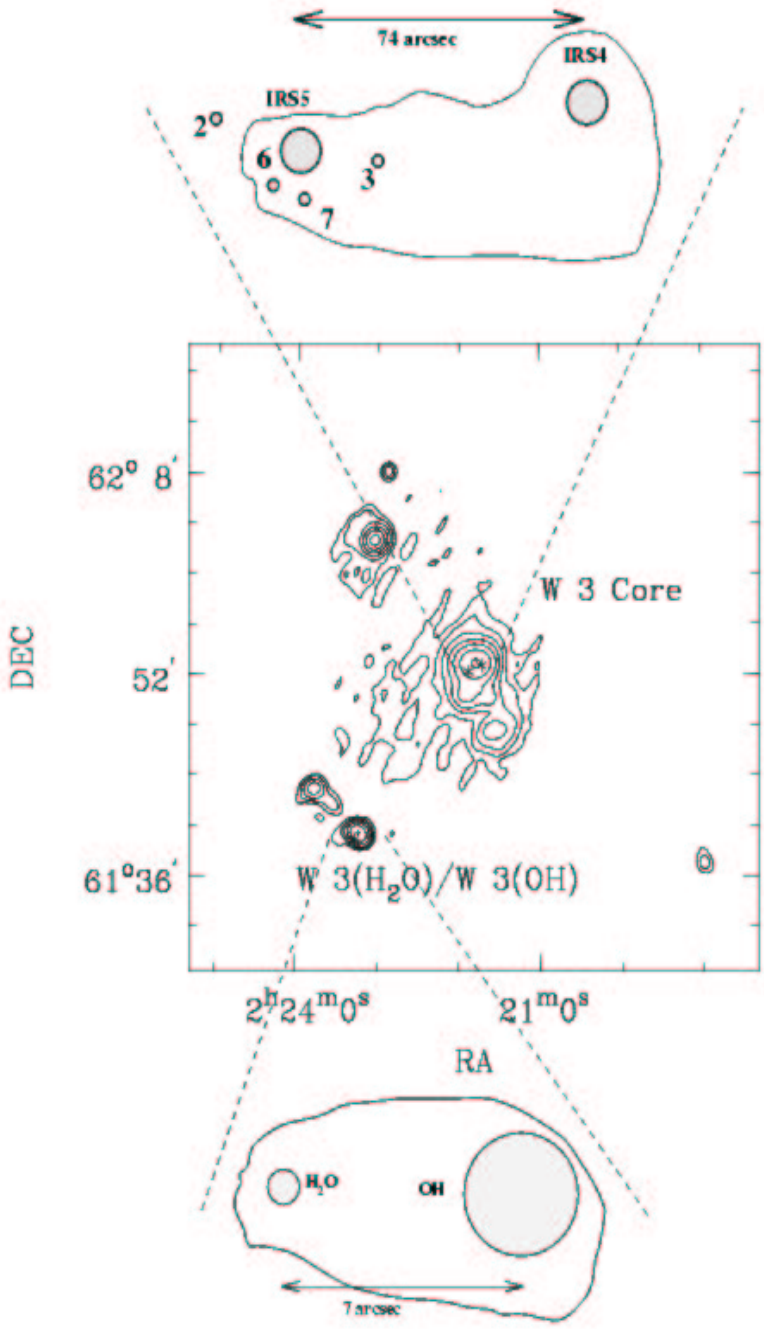

Figure 1: Middle: high resolution 25 μm IRAS map of the W 3 GMC region, prepared by P. Roelfsema SRON Groningen). The center core is W 3(Main). W 3(Main) is shown in more detail in the cartoon at the top. IRS 2 to 7 are indicated. In the cartoon below the compact HII region W 3(OH) and the "hot core" W 3(H_2O) are shown.

Interstellar Dust Clouds) will be discussed. The model is implemented in the program CSDUST3 from Egan et al. (1988). CSDUST3 will be discussed in Section 3.2. Important aspects to the model and code are radiative transport, dust, internal radiation field, interstellar radiation field, spatial grid and wavelength grid.

The problem is solved by determining the equilibrium dust temperature. This is done by determining the combined moment equations of radiative transport, cast in a quasi-diffusion form. The result is a boundary value problem for a second order differential equation, which is solved by the method of finite differences. The resulting non-linear system is solved by use of the Newton-Raphson method. For further details on the Newton-Raphson method and solving the problem see (e.g. Leung, 1976a) and Burden & Faires (2001).

2.1 Model

2.1.1 Radiative Transport

The equation of radiative transfer, written in spherical/cylindrical geometry is given by Eq. (2.1) below. The meaning of the symbols are given in Table 8 in Appendix A.

$$\mu\frac{\partial I_\nu(r,\mu)}{\partial r}+\frac{m}{2}\left[\frac{1-\mu^2}{r}\frac{\partial I_\nu(r,\mu)}{\partial \mu}\right] = \overbrace{-\sigma_\nu^a(r)[I_\nu(r,\mu)-\underbrace{B_\nu(r)}_{\text{Planck}}]}^{\text{emission - absorption}} \underbrace{-\sigma_\nu^s(r)[I_\nu(r,\mu)-\frac{1}{2}\int_{+1}^{-1} I_\nu(r,\mu')p_\nu(\mu,\mu')\mathrm{d}\mu'}_{\text{scattering}} \tag{2.1}$$

The first step in solving (2.1), is expanding the phase function ($p_\nu(\mu,\mu')$) in a series of Legendre polynomials (Chandrasekhar 1960)

$$p_\nu(\mu,\mu') \approx \sum_{l=0}^{L} a_l P_l(\mu) P_l(\mu') \tag{2.2}$$

Here only the first two terms are taken into account. The second step is defining the moments of the radiation field

$$M_\nu^n(r) \equiv \frac{1}{2}\int_{-1}^{+1} I_\nu(r,\mu)\mu^n \mathrm{d}\mu \tag{2.3}$$

The first three moments $J_\nu \equiv M_\nu^{n=0}(r)$, $H_\nu \equiv M_\nu^{n=1}(r)$ and $K_\nu \equiv M_\nu^{n=2}(r)$, are respectively the mean intensity, the Eddington flux and the K-integral. Using the moments Equation (2.1) is rewritten into

$$\boxed{\frac{\partial}{\partial r}\left(\frac{r^m}{\kappa_\nu\zeta_\nu}\frac{\partial(f_\nu\zeta_\nu J_\nu)}{\partial r}\right) = r^m(\kappa_\nu^* J_\nu - \epsilon_\nu^*)} \tag{2.4}$$

where

$$\zeta_\nu(r) = \begin{cases} 1 & \text{for cylindrical geometry} \\ e^{\int_{r_c}^{r}\left[3-\frac{1}{f_\nu(x)}\right]\frac{\mathrm{d}x}{x}} & \text{for spherical geometry} \end{cases} \tag{2.5}$$

and

$$f_\nu(r) \equiv \frac{K_\nu}{J_\nu} \tag{2.6}$$

The meaning of the symbols are given in Table 9 in Appendix A.

The function $f_\nu(r)$ is called the anisotropy factor, a measure of the anisotropy of the radiation field. $\zeta_\nu(r)$ is called the configuration function which is a measure for the geometry. In the Eddington approximation $f_\nu(r) = \frac{1}{3}$ and $\zeta_\nu(r) = 1$. The Eddington approximation is exact for isotropic radiation and exact when for every τ_ν $I_\nu(\tau_\nu, \mu)$ can be expanded, in only odd powers of μ, in the serie $\sum_{i=0}^{n} a_i(\tau_i)\mu^i$. This is when for all even coefficients $a_i = 0$ (see Rutten (1995)).

Step three is using the two stream approximation, taken from Ribicky & Lightman (1985). Then the boundary conditions on equation (2.4) are set to

$$\frac{\partial}{\partial r}(f_\nu \zeta_\nu J_\nu) = \kappa_\nu \zeta_\nu (2H_\nu^- - f_\nu^{\text{boundary}} J_\nu) \text{ at } r = R \tag{2.7a}$$

$$\frac{\partial}{\partial r}(f_\nu \zeta_\nu J_\nu) = -\kappa_\nu \zeta_\nu H_\nu^* \text{ at } r = r_c \tag{2.7b}$$

H_ν^* is the inner flux that follows from the central source and will be discussed in section 2.1.3. H_ν^- is the incident flux that follows from the interstellar radiation field. The interstellar radiation field will be discussed in section 2.1.4.

When the Eddington approximation is used, the radiative transport problem is solved by solving the combined moment equations (2.3). The boundary conditions are then set by (2.7a) and (2.7b).

When the Eddington approximation is not used, $I_\nu(r, \mu)$ at each wavelength must also be determined to evaluate $f_\nu(r)$. This is done by using the ray-tracing method. This means in the case of spherical geometry that a transformed coordinate system (r, ξ) is introduced, see Fig. 2.

$$\xi = r\sin(\theta) = r\sqrt{(1-\mu^2)} \Longleftrightarrow \mu = \pm\sqrt{1 - \left(\frac{\xi}{r}\right)^2} \tag{2.8}$$

In the fourth step I_ν has been separated into a I_ν^+ and a I_ν^- component. This is possible because of the double value of μ. If now u_ν and v_ν are defined as

$$u_\nu \equiv \frac{1}{2}(I_\nu^+ + I_\nu^-) \tag{2.9}$$

$$v_\nu \equiv \frac{1}{2}(I_\nu^+ - I_\nu^-) \tag{2.10}$$

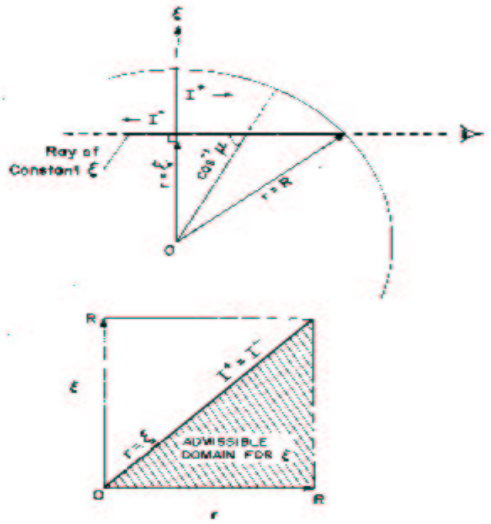

Figure 2: Top: overview of the variables r, μ, ξ and the classification of intensities I_ν^+ and I_ν^- in the physical plane. Bottom: Admissible domain for ξ, the impact parameter in the (r, ξ)-plane. (Figure taken from Leung (1975).)

the moments can be re-written into

$$J_\nu(r) = \int_0^1 u_\nu(r,\mu)\mathrm{d}\mu \tag{2.11}$$

$$H_\nu(r) = \int_0^1 v_\nu(r,\mu)\mu\mathrm{d}\mu \tag{2.12}$$

$$K_\nu(r) = \int_0^1 u_\nu(r,\mu)\mu^2\mathrm{d}\mu \tag{2.13}$$

and Eq. (2.1) into the two components I_ν^+ and I_ν^-

$$\mu\frac{\partial I_\nu^+}{\partial r} = -(\sigma_\nu^\alpha + \sigma_\nu^s)(I_\nu^+ - S_\nu) \tag{2.14}$$

$$\mu\frac{\partial I_\nu^-}{\partial r} = (\sigma_\nu^\alpha + \sigma_\nu^s)(I_\nu^- - S_\nu) \tag{2.15}$$

where the Source Function S_ν is defined as

$$S_\nu(\mu) \equiv \frac{1}{(\sigma_\nu^\alpha + \sigma_\nu^s)}\Big[\frac{\sigma_\nu^s}{2}\int_{-1}^1 I_\nu(\nu')p_\nu(\mu,\mu')\mathrm{d}\mu' + \sigma_\nu^\alpha B_\nu\Big] \tag{2.16}$$

In the fifth step, by alternately adding and subtracting (2.14) and (2.15), two second-order differential equations are found from which v_ν can be eliminated. The exercise results into

$$\frac{\mu}{\sigma_\nu^\alpha + \sigma_\nu^s}\frac{\partial}{\partial r}\Big(\frac{\mu}{\sigma_\nu^\alpha + \sigma_\nu^s}\frac{\partial \mu_\nu}{\partial r}\Big) = u_\nu - S_\nu \tag{2.17}$$

which is linear in u_ν.

When solving the problem numerical with the Newton-Raphson method a first iteration step is needed. The Source Function can be used for this, when assuming isotropic scattering. S_ν is in that case given by

$$S_\nu = \frac{\sigma_\nu^s J_\nu + \sigma_\nu^\alpha B_\nu}{\sigma_\nu^s + \sigma_\nu^\alpha} \tag{2.18}$$

For anisotropic scattering the scattering term is rewritten into

$$\frac{1}{2}\int_{-1}^{1} I_\nu(\mu')p_\nu(\mu,\mu')\mathrm{d}\mu' = \int_0^1 \left[p_\nu^+(\mu,\mu')u_\nu(\mu') + p_\nu^-(\mu,\mu')v_\nu(\mu')\right]\mathrm{d}\mu' \tag{2.19}$$

in which

$$p_\nu(\mu,\mu') = p_\nu^+(\mu,\mu') + p_\nu^-(\mu,\mu') \tag{2.20}$$

The radiative transport problem in general has now been solved, but for the determination of the dust temperature, dust parameters must be included.

2.1.2 Dust

For the dust radiative equilibrium is set, neglecting loss of energy through non-radiative transfer

$$\int_0^\infty (\epsilon_\nu^* - \kappa_\nu^* J_\nu)\mathrm{d}\nu = 0 \tag{2.21}$$

Written in a more common form and using the Mie scattering theory the previous equation becomes

$$\int_0^\infty J_\nu(r)\langle Q_{\mathrm{abs}}\pi a^2\rangle_\nu \mathrm{d}\nu = \int_0^\infty B_\nu[T(r)]\langle Q_{\mathrm{abs}}\pi a^2\rangle_\nu \mathrm{d}\nu \tag{2.22}$$

Where the quantity $\langle Q_{\mathrm{abs}}\pi a^2\rangle_\nu$ is weighted for a mixture of grain sizes. The efficiency factor Q_{abs} can be determined from the extinction coefficient and the albedo using the relations given below,

$$C_{\mathrm{extinction}} = C_{\mathrm{scattering}} + C_{\mathrm{absorption}} \tag{2.23a}$$

$$\mathrm{albedo} = \frac{C_{\mathrm{scattering}}}{C_{\mathrm{absorption}}} \tag{2.23b}$$

$$C_{\mathrm{absorption}} = Q_{\mathrm{absorption}}\pi a^2 \tag{2.23c}$$

$$C_{\mathrm{scattering}} = Q_{\mathrm{scattering}}\pi a^2 \tag{2.23d}$$

with a the grain size. Usually the quantities presented in grain models for the scattering coefficient are already weighted with a grain size distribution.
It is sometimes common and convenient to write the extinction coefficient in terms of 'per Hydrogen Nucleon'; $C_{\mathrm{extinction}}/\mathrm{H}$. Doing this only changes the grain number density ($n(r)$) into a Hydrogen number density ($n_{\mathrm{H}}(r)$).

The total number of dust particles is determined through a specified optical depth τ at a specified wavelength.

$$N = \frac{\tau_\lambda}{C_{\text{extinction}}}$$

For given N the density distribution is fitted e.g. a power law ($n(r/R) = n_0\left[\frac{r}{R}\right]^{-\gamma}$). When the extinction coefficient is provided 'per Hydrogen nucleon', instead of 'per grain', the total number of Hydrogen nucleons is determined.
There are no effects on the radiative transfer since the energy balance doesn't change. In equation 2.22 the effects are taken out since the constant conversion factor can be put outside the integrals and divided out.

Furthermore, in Mie scattering theory the second term of the Legendre approximation, Eq. (2.2), called g is determined

$$g = \frac{1}{2}\int_{-1}^{+1} p_\nu(\alpha)\alpha \mathrm{d}\alpha \tag{2.24}$$

The model is able to handle different dust models and grain size distributions.

2.1.3 Internal Radiation Field

For the central heat source the flux of a blackbody with temperature T_* is assumed. Then the total luminosity is given by

$$L_* = 4\pi r_*^2 \int_{\nu_{\min}}^{\nu_{\max}} B_\nu(T_*)\mathrm{d}\nu \tag{2.25}$$

and the net flux by

$$H_\nu^* = \frac{1}{4}\left(\frac{r_*}{r}\right)^2 B_\nu(T_*) \tag{2.26}$$

2.1.4 Interstellar Radiation Field

The intensity from the interstellar radiation field can be represented by a sum of several diluted blackbody spectra

$$I_\nu^-(R) = \sum_i W_i B_\nu(T_i) \tag{2.27}$$

where W_i is a dilution factor and $B_\nu(T_i)$ is the Planck function for a temperature T_i. The incident flux at the boundary then becomes

$$H_\nu^-(R) = \frac{1}{2}\int_0^1 I_\nu^-(R)\mu \mathrm{d}\mu = \frac{1}{4} I_\nu^-(R) \tag{2.28}$$

Fig. 3 shows for example the interstellar radiation field with values for W_i and T_i presented by Mathis et al. (1983). Mathis et al. (1983) use three diluted blackbodies with temperatures T_i is 7500 K, 4000 K, 3000 K and a non-diluted blackbody for the Cosmic Microwave Background at a temperature of 2.8 K (Werner and Salpeter 1969). The three dilution factors are respectively $1 \cdot 10^{-14}$, $1 \cdot 10^{-13}$ and $4 \cdot 10^{-13}$.

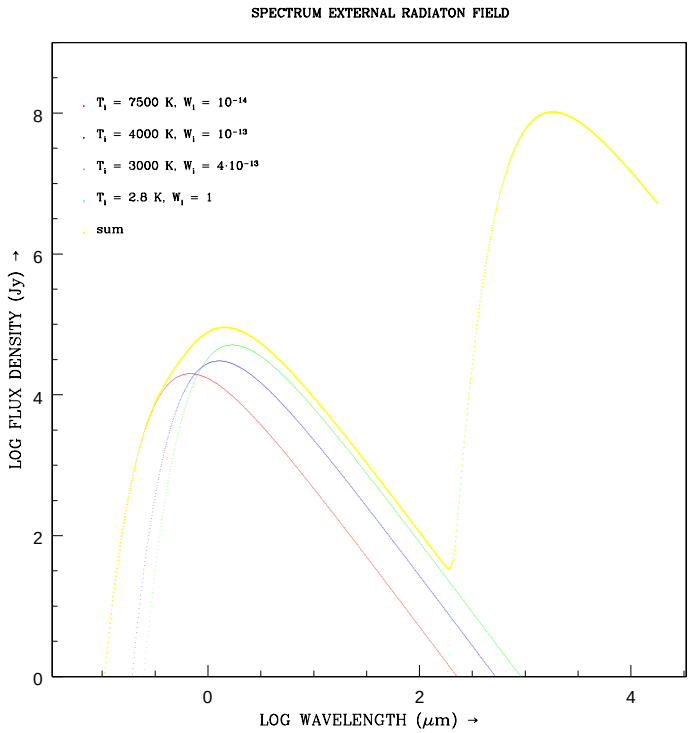

Figure 3: Modeled interstellar radiation field consisting of three diluted blackbodies and a one non-diluted blackbody for the Cosmic Microwave Background. Values for T_i and W_i are taken from Mathis et al. (1983)

The set of equations has been completed and can be solved. Solving the problem is done on a spatial grid and a wavelength grid, which will be discussed in the next two subsections.

2.1.5 Spatial grid

As usual in most finite-difference problems the choice of the grid on which the problem is solved is very important. The success of the iterative scheme can even depend on it. Special attention should be given to the boundary since it is a boundary problem that has to be solved.
It is recommended to have an approximately logarithmic distribution of points with extra points near the center ($r \approx r_c$) and at the edge of the cloud ($r \approx R$). In this way rapid changes near the boundaries can be dealt with.

When scaling the problem down on a grid in the range $[0-1]$ having 100 points, a continuous function, say $f(x)$, can be used to map the range $[0-99]$ onto $[\frac{r_c}{R}-1]$. $\frac{r}{R}$ is then the inner core radius, if an inner cavity is present. The speed of change in the step size Δr, is approximately given by the derivative.

$$\Delta r \approx \frac{\mathrm{d}f(x)}{\mathrm{d}x} \tag{2.29}$$

For example take $f(x) \propto x^{\alpha}$; $f(x) = (1-\frac{r_c}{R})\left(\frac{x}{99}\right)^{\alpha}+\frac{r_c}{R}$. The step size is then approximately given by $\Delta r \propto \alpha \cdot x^{\alpha-1}$, if $\alpha \neq 0$. Mappings for $\alpha = 1, 2, 3$ and 4 are plotted in Fig. 4.

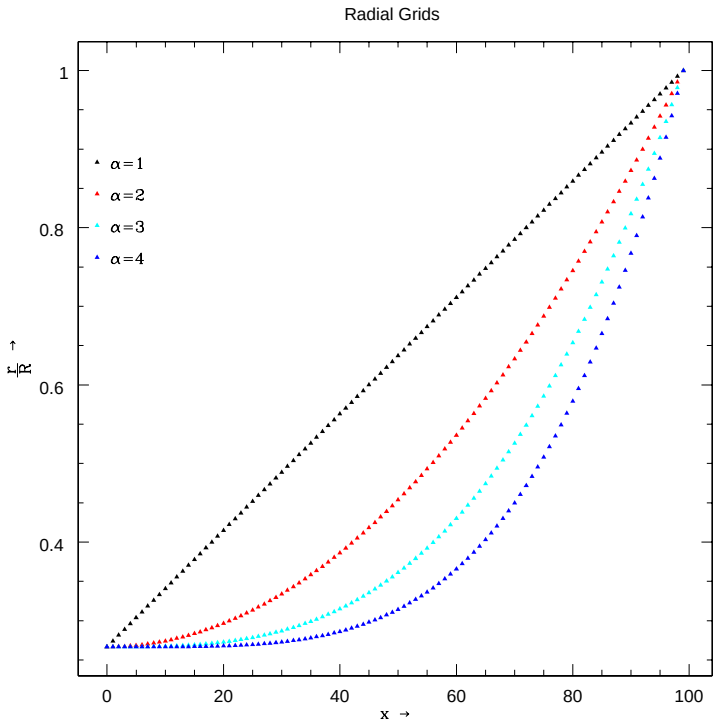

Figure 4: Radial grid mappings for $f(x) = (1 - \frac{r_c}{R})\left(\frac{x}{99}\right)^{\alpha} + \frac{r_c}{R}$, with four different exponents α.

In general the following can be stated for the spatial grid

- When the opacity varies over a small distance for a certain dust component, the grid should be finer there.
- The overall step size should never be too great.
- Near the two boundaries the grid spacing should approximately correspond to the step size of the optical depth.
- Models with a high optical depth or steep density gradient require a finer grid. In our case the optical depth is high and a relatively fine grid is required.

2.1.6 Wavelength Grid

The set of equations can, on its own, be solved on the entire frequency spectrum. However the results for very short and very long wavelengths wouldn't present a realistic picture. CSDUST3 can handle a broad spectrum from $\lambda_{\text{min}} = 0.1$ μm up to $\lambda_{\text{max}} = 10^4$ μm. Assumed is that everything below the $\lambda = 912$ Å Lymann edge is to be degraded into low-energy photons beyond the Lyman limit.
Wavelengths of own choice can be incorporated into the grid, for example specific wavelengths at which observed data is available. At least a few Ultra Violet (UV) up to some

optical wavelength should be included, required for grain heating.

2.1.7 Beam Convolution

Beam convolution is useful for making comparison between the results from the model and observed date. Convolution is done by

$$\int_{\theta=0}^{2\pi}\int_{r=0}^{\infty} I(r,\theta)G(r,\theta)r\mathrm{d}r\mathrm{d}\theta \tag{2.30}$$

The assumption is that the beam pattern is circular symmetric and Gaussian so that

$$G = G(r) \propto e^{\frac{-r^2}{2\sigma^2}} \tag{2.31}$$

σ is the half width of the beam and is expressed as a fraction of the source size. The sizes of beams are usually given in $''$ and need to be converted into a fraction of the source size. If, say, ϵ is the half width of the beam in $''$, σ can be calculated using the following relation

$$\sigma = \frac{\epsilon}{\arctan\left(\frac{R}{D}\right)} \tag{2.32}$$

here R is the radius of the object, in our case the radius of IRS 5 and D is the distance to the object. If the beam widths are presented as FWHM (Full Width at Half Maximum) also the following relation has to be used to make the conversion to σ

$$\mathrm{FWHM} = \sigma\sqrt{8\ln 2} \approx 2.3548\sigma \tag{2.33}$$

Combining both conversions results into

$$\sigma = \frac{\epsilon}{\arctan\left(\frac{R}{D}\right)\cdot\sqrt{8\ln 2}} \tag{2.34}$$

Carrying out the integration (2.30) over r numerical, an upper limit of 4σ should be sufficient.

$$\frac{1}{2\pi\sigma^2}\int_{\theta=0}^{2\pi}\int_{r=0}^{4\sigma} I(r,\theta)e^{\frac{-r^2}{2\sigma^2}}r\mathrm{d}r\mathrm{d}\theta \tag{2.35}$$

2.2 Software

The program implementing the model from Leung (1975, 1976b) is CSDUST3 from Egan et al. (1988). The program is written in FORTRAN77 and it can be downloaded from the CPC Program Library at
http://www.cpc.cs.qub.ac.uk/cpc/astro.html. To make the program run on a Linux platform two adjustments had to be made

1. In the **OPENFL** subroutine, which handles the file opening, the PARM='PRINT' argument to **OPEN** had to be changed into **PARM='FORMATTED'**
2. In the **EXPOFF** subroutine, which handles the number under/overflow, the **CALL SIGNAL(8,QQ,1)** line was commented out.

Documentation on Fortran 77 shows that the normalized double-precision floating-point value is in the approximate range of $(2.225074D-308, 1.797693D+308)$. In our case this should be more than enough.
Compiling the program and running it with the test input data, included in the download, showed no differences when comparing it to the output presented by Egan et al. (1988).

The next task was finding out what the parameters in the input and output file are. The parameters for the input are listed in Table 10 in Appendix B.1. An example of an input file is given in Appendix B.2. In Appendix C.1 in Table 11 the output parameters and their meaning are given. An example of an output file is given in Appendix C.2. A more extended discussion on the input parameters and their values will be given in section 3.4. A short discussion on some of the output parameters is given in section 4.

For the interaction with CSDUST3, especially in handling the input/output, a simple user interface program BuI (Boersma user Interface) has been written. BuI is able to give direct graphical representation of some of the parameters e.g. the dust number density distribution and the temperature distribution. BuI is written in C++, with the use of the PGPLOT library for handling the plot routines. A screen shot of BuI is shown in Fig. 5 and the flowchart of the program is shown in Fig. 7.

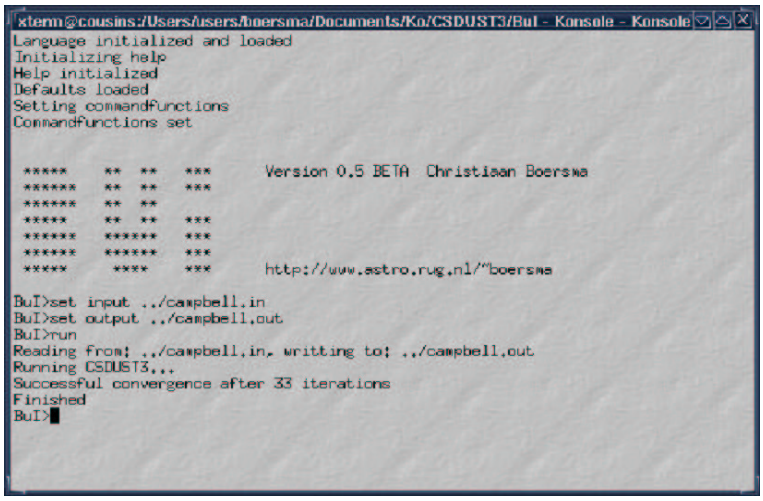

Figure 5: Screen shot of BuI (Boersma user Interface), program written around CSDUST3 for handling input,output and plotting.

When a power law for the density is chosen, $n(r) \propto r^{-\gamma}$ where γ is the power law index, an inner Gaussian is fitted to avoid the singularity at $r = 0$. CSDUST3 fits the inner Gaussian and the power law at the point where 80% of the total optical depth occurs within the power law region.
In our case there is a cavity at the center of the cloud, so a singularity at $r = 0$ is already avoided. However in the general case, for better profiles CSDUST3 has been adapted to fit the inner Gaussian and the power law at the point where 99% of the optical depth occurs within the power law. This meant changing **ALPHA=0.8** in line 539 of the sourcecode into **ALPHA=0.99**. The difference in the results for the dust number density distribution

are shown in Fig. 6.

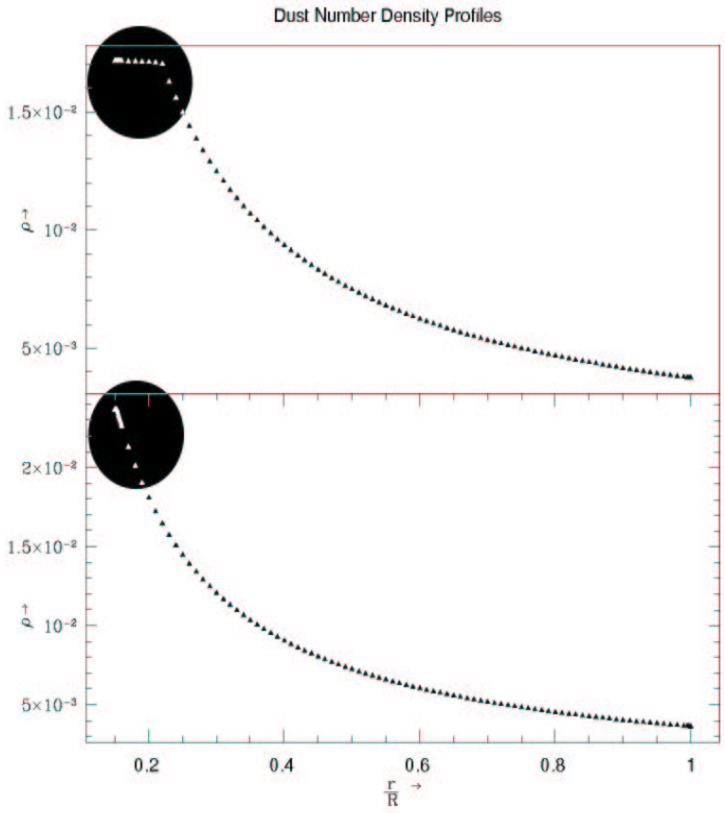

Figure 6: Dust Number Density Profiles; Density is power law with index 1. Top: inner Gaussian fit to the power law at the point where 80% of the optical depth occurs within the powerlaw. Bottom: inner gaussian fit to the powerlaw at the point where 99% of the optical depth occurs within the powerlaw .

Input to CSDUST3 are a radial and wavelength grid, information on the interstellar radiation field at each wavelength point, object properties e.g. luminosity, further absorption and scattering cross sections for each grain type at each wavelength point and the scattering asymmetry parameter g for each grain type at each wavelength point. When doing the beam convolution to make comparison with observed data, also the half beam widths (σ) for the assumed circular Gaussian beam pattern ($G(r) \propto e^{\frac{-r^2}{2\sigma^2}}$) at each wavelength should be provided.

CSDUST3 is able to handle 100 grid points, 60 wavelength points and up-to 6 different grain types. The selection of the half beam widths for each wavelength makes it possible to do direct comparisons with data at the same wavelength from different telescopes with different beam widths. However convolution can also be done afterwards by 'hand'.

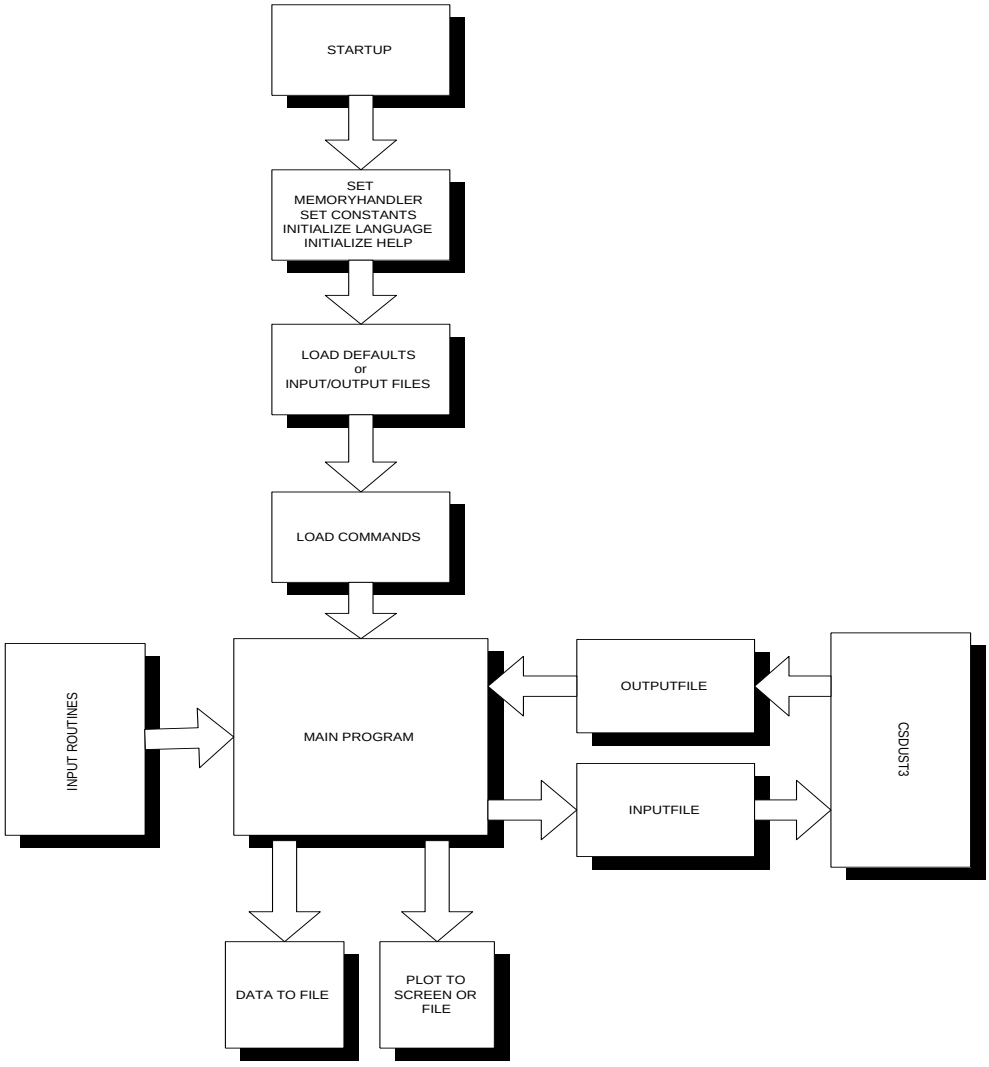

Figure 7: Flowchart of the user interface program BuI (Boersma user Interface) showing the different parts of the program.

3 Data

The results to which comparisons are made and some of the input data to CSDUST3, are obtained from Campbell et al. (1995), the dust parameters are taken from a model developed by Weingartner & Draine (2001) and Li & Draine (2001) and the interstellar radiation field parameters are assumed to be those from Egan et al. (1988). The focus is on trying to reproduce the Spectral Energy Distribution (SED) from Campbell et al. (1995), which is shown in Fig. 8, which is the main test for the found procedure.
Campbell et al. (1995) present four different models which they tried to fit with the observed data. Model 3 is used for comparison with our work. Arguments for using model 3 were the presence of an inner core, model 3 uses the dust model from Draine & Lee (1984) and it has the lowest reduced χ^2 at 47 μm (36$''$ beam).

Required data for the model are the properties of the object W 3 IRS 5, dust parame-

ters and interstellar radiation field parameters, which are discussed below. Although not relevant here, since the focus is on a procedure and not on the explanation of observed data, the observed fluxes with their uncertainties are presented in Table 5, which is taken from Campbell et al. (1995).

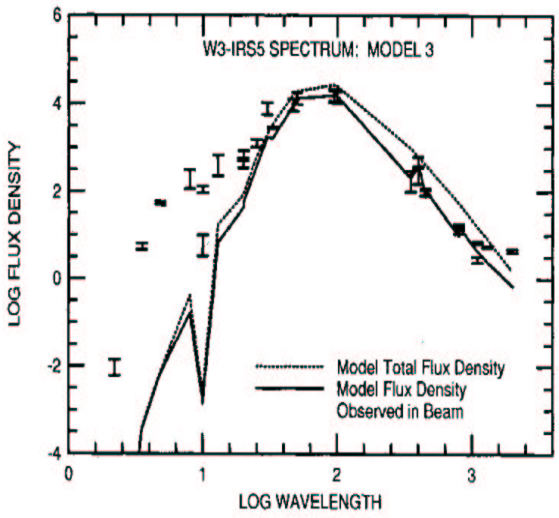

Figure 8: Spectral Energy Distribution (SED) from Campbell et al. (1995), the main test for the found procedure. WAVELENGTH is in units of μm and the FLUX DENSITY is in units of Jy

The necessary steps to create the input file for CSDUST3, which is actually the procedure, are presented in section 3.4.

3.1 W 3 IRS 5

The properties of the object W 3 IRS 5 where already presented in section 1.2 Table 3, together with properties of model 3 from Campbell et al. (1995), the are presented again in Table 4.

Luminosity of stars	$2.5 \times 10^5\ L_\odot$
Temperature of stars	25,000 Kelvin
Distance	2.3 kpc
Cloud outer radius, R	0.35 pc
Cloud cavity radius r_c	0.08 pc
Exponent in density power law, γ	-1.0
Optical depth at 95 μm (r_c - R)	0.30
Dust properties	Draine & Lee

Table 4: Properties and model parameters for W 3 IRS 5, taken from Campbell et al. (1995) Table 1.

Wavelength (μ)	F_ν (Jy)	Uncertainty (Jy)	Beam $''$
2.2	0.01	0.004	10
3.5	5.4	0.9	10
4.8	54	5	10
8	213	100	7.5
10	112	19	10
10	6.6	3.3	7.5
13	450	225	7.5
30	427	80	10
30	719	143	13.5
25	1290	260	13.5
33	2865	165	13.5
30	8200	2460	30
47	9800	2900	22
50	14000	4200	30
95	15000	4600	28
95	16900	5100	30
100	15000	4500	30
350	200	100	15
400	250	100	35
400	500	125	49
450	81	2	14
450	112	3.4	17.5
800	13.9	0.3	14
800	15	1.1	14
800	17	1.3	16
800	13.5	2.7	19
1100	6.8	0.46	18.5
1100	2.75	0.4	19
1300	5.5	0.32	19.5
2000	4.4	0.44	27.2

Table 5: Observed photometric data for W 3 IRS 5, taken from Campbell et al. (1995) Table 2, although not relevant for the research 'an sich' presented here for completeness

3.2 Dust

There is deviation from the model properties as presented in Table 4. For the dust properties the results from a grain model developed by Weingartner & Draine (2001) and Li & Draine (2001) is used instead of that from Draine & Lee (1984). The model used now has a mixture of carbonaceous and silicate grains to produce synthetic extinction curves. The produced curves have been proved to be in agreement with observed interstellar extinction, scattering and infrared emission.

Tabulated results for extinction, albedo, and absorption cross sections are available at: http://www.astro.princeton.edu/∼draine/dust/dustmix.html. Due to lack of better data the $R_V = 3.1$ data is taken. The presented data for the extinction coefficient is given per hydrogen nucleon.

Relations (2.23a) - (2.23d) in section 2.1.2 are used to rewrite the tabulated data into the form needed for the input file for CSDUST3. The dust parameters needed for the input file are $Q_{\text{absorption}}\pi a^2$, $Q_{\text{scattering}}\pi a^2$ and g at each wavelength. Presenting the parameters per hydrogen nucleon only changes the dust number density ($n(r)$) into a Hydrogen number density (n_{H}), see section 2.1.2. The tabulated data is linearly interpolated on the wavelength grid. In Fig. 9 respectively the absorption cross-section, the scattering cross-section and the scattering asymmetry parameter g are plotted against wavelength. The data below 912 Å is not used since CSDUST3 assumes that those photons are all converted into low-energy photons.

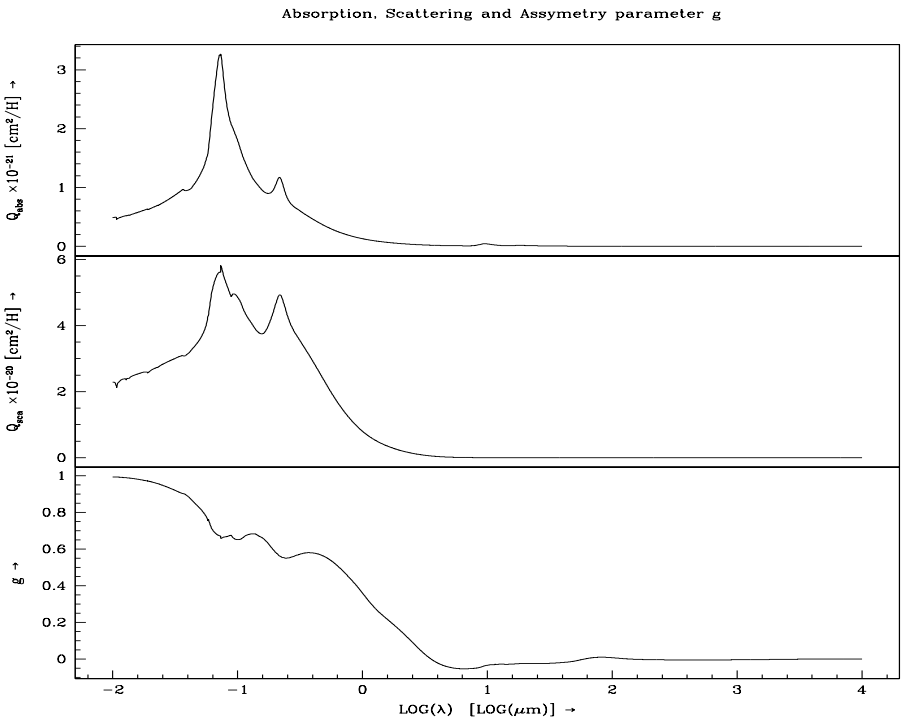

Figure 9: Plotted absorption cross-section, scattering cross-section and scattering asymmetry parameter g as function of wavelength from [0.02 - 10.000] μm.

3.3 Interstellar Radiation Field

It is not clear whether Campbell et al. (1995) use an interstellar radiation field, however for the completeness of the procedure it is used here. Leung (1975, 1976b) mention an interstellar radiation field consisting of the sum of three diluted blackbodies and a non-diluted 2.8 Kelvin blackbody for the isotropic cosmic microwave background. The three dilution factors W_i and the three temperatures T_i (see (2.1.4), section 2.1.4) are not presented by Leung (1975, 1976b). Neglected by Leung (1975, 1976b) are the very far infrared radiation from the galactic center and possible contributions from T-Tauri stars, which are preferentially located near dark clouds. The data on the interstellar radiation field presented in the trial input file is used here and it is assumed that it is based on the model presented by Leung (1975, 1976b). The data on the interstellar radiation field from the trial input file is plotted in Fig. 10. For the input to CSDUST3 the data is linearly interpolated on the wavelength grid. Taking a look at Fig.10 immediately raises questions if the radiation field presented in the trial input file is real and if it is that discussed by Leung (1975, 1976b).

3.4 Input CSDUST3

Now the long write-up of the input file, which could be interpreted as the procedure. The choices made are also discussed. It is tried is to stay as close as possible to the Campbell et al. (1995). Additional information on the parameters can be found in Appendix B.1 Table 10.

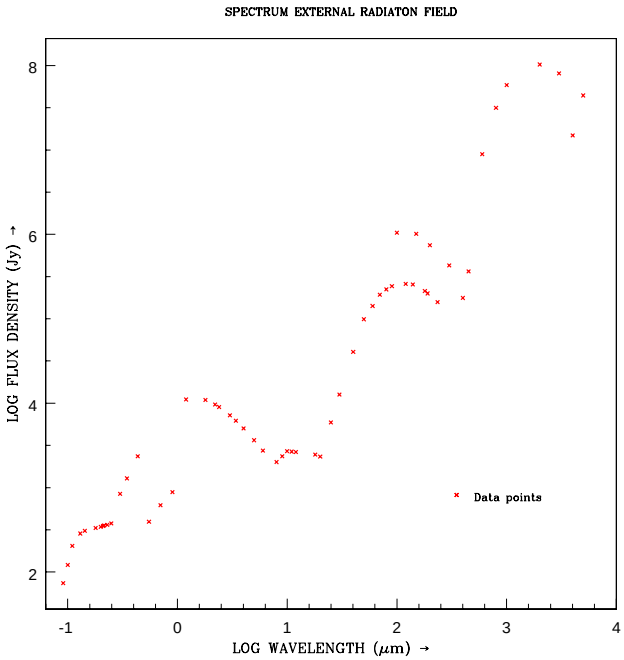

Figure 10: Plotted data on the interstellar radiation field taken from the trial input file. Assumed is that the data is from the model presented by Leung (1975, 1976b)

NUMBER OF MODELS
One model is run. There is the option to put more than one model, with the same dust model and boundary characteristics, into a single input file. The different models are then run successively.
(*NMODEL = 1*)

GEOMETRY
Slab, cylindrical and spherical geometry can be chosen. As Campbell et al. (1995) spherical geometry is assumed.
(*IEMERG = 2*)

NUMBER OF ANGLES FOR EMERGENT INTENSITIES
The number of angles at which the emergent intensities are calculated in the cylindrical case can be given in. The option is four or one angle. Since in our case the geometry is not cylindrical the value doesn't matter and is put on 1, which is the value for four angles.
(*IGEOM = 1*)

THE USE OF THE EDDINGTON-APPROXIMATION
The Eddington-approximation can be used when solving the emergent intensity. Using the Eddington-approximation would result in a faster computation. However when using modern high-speed computers the gain in time would be minimal. Nevertheless still the Eddington-approximation is used since the difference in the results would be minimal.
(*IEDFTR = 0*)

OUTPUT
A detailed or a simple printout of the characteristics of the radiation field can be chosen. The detailed print out is chosen, since it contains the information needed to construct the Spectral Energy Distribution (SED).
(*IOUT = 1*)

CENTRAL CORE
The presence of a central core can be specified. Here a central core is present; IRS 5.
(*IC = 1*)

TOTAL NET FLUX AT CORE
The flux from the central heat source can be treated as a net flux or as the incident flux. Egan et al. (1988) indicate that for optically thick media both choices give rather similar results. Since the medium here is optically thick it doesn't matter much which choice is made. Therefore the value from the test input file is adopted; treat the flux from the central heat source as net flux.
(*NH = 1*)

FIRST ORDER SCATTERING
First order anisotropic scattering or isotropic scattering can be chosen. The dust data used here include the scattering asymmetry parameter g, therefore for realistic modeling the anisotropic scattering is used. Anisotropic scattering would require more computing time, but on modern high-speed computers the gain in time is negligible.
(*ISCA = 1*)

INCIDENT FLUX AT OUTER BOUNDARY
It is not clear from Campbell et al. (1995) if they use an interstellar radiation field at the outer boundary. For realistic modeling and for completeness of the procedure an interstellar radiation field at the outer boundary is used.
(*IB = 1*)

DUST DISTRIBUTION
The dust density distribution can be chosen a power law or Gaussian. In line with Campbell et al. (1995) the power law is chosen.
(*IDIST = 0*)

NORMALIZATION CONSTANT
The normalization constant for the intensity is to prevent numerical underflow or overflow. The normalization constant is taken 10^{-30}, the same as in the test input file and it seems to be sufficient
(*AJ0 = 1.000D-30*)

MAXIMUM FRACTIONAL ERROR ALLOWED FOR CONVERGENCE
Convergence is achieved when two criteria are met. First at each point the heating and cooling rates for the dust grains must be equal. Secondly flux conservation should hold both globally and locally. The maximum fractional error allowed for convergence parameter sets the tolerance in the equality requirements. The maximum fractional error allowed for convergence is set on 10^{-3}, the same as in the test input file and it seems to be sufficient.
(*EPS = 1.000D-03*)

MAXIMUM NUMBER OF ITERATIONS
More complex models and different geometries take longer to converge. Egan et al. (1988) predict in the order of 10 iterations, therefore the maximum number of iterations in the test input file is set on 20, which a first glance should be sufficient. However after running the program it showed that more iterations were required and since with the use of high speed computers the extra time needed to do more iterations is small, the maximum number of iterations is set to 35.
(*ITMAX = 35*)

OUTER CLOUD RADIUS
The outer cloud radius is set to 0.35 pc (see Table 4).
(*RMAX = 0.350D 00*)

SPATIAL GRID
Campbell et al. (1995) don't mention the spatial grid on which they run CSDUST3. Here a spatial grid $\propto r^3$, $\alpha = 3$, is used and core radius $r_c = 0.08$ pc, see section 2.1.5. In the first few grid points the step size is taken 0.0001 because the maximum precision is smaller than the step size of the power law.
(*NR(R) =*

```
2.229d-01 2.230d-01 2.231d-01 2.234d-01 2.238d-01 2.244d-01 2.251d-01
2.259d-01 2.268d-01 2.280d-01 2.292d-01 2.306d-01 2.321d-01 2.338d-01
2.357d-01 2.377d-01 2.398d-01 2.421d-01 2.446d-01 2.472d-01 2.499d-01
2.528d-01 2.559d-01 2.591d-01 2.625d-01 2.661d-01 2.698d-01 2.737d-01
2.777d-01 2.819d-01 2.862d-01 2.907d-01 2.954d-01 3.003d-01 3.053d-01
3.104d-01 3.158d-01 3.213d-01 3.269d-01 3.328d-01 3.388d-01 3.449d-01
3.513d-01 3.578d-01 3.644d-01 3.713d-01 3.783d-01 3.855d-01 3.928d-01
4.003d-01 4.080d-01 4.159d-01 4.239d-01 4.321d-01 4.405d-01 4.491d-01
```

```
4.578d-01 4.667d-01 4.757d-01 4.850d-01 4.944d-01 5.040d-01 5.137d-01
5.237d-01 5.338d-01 5.441d-01 5.546d-01 5.652d-01 5.760d-01 5.870d-01
5.982d-01 6.095d-01 6.210d-01 6.327d-01 6.446d-01 6.567d-01 6.689d-01
6.813d-01 6.939d-01 7.067d-01 7.196d-01 7.328d-01 7.461d-01 7.596d-01
7.732d-01 7.871d-01 8.011d-01 8.153d-01 8.297d-01 8.443d-01 8.590d-01
8.740d-01 8.891d-01 9.044d-01 9.199d-01 9.355d-01 9.514d-01 9.674d-01
9.836d-01 1.000d+00)
```

NUMBER OF WAVELENGTH POINTS
Campbell et al. (1995) present 30 wavelength points in Table 2 of their paper. The number of wavelength points they use as input is not mentioned. Here all 30 wavelength points are included plus 13 UV through visible wavelength points (between $1.0 \cdot 10^{-2} - 7.0 \cdot 10^{-1}$ μm) and 17 intermediate points in the infrared range. This adds up to the maximum allowed number of wavelength points of 60. (*NFD = 60*)

WAVELENGTH GRID
The wavelength grid is in μm. It runs from 9.1×10^{-2} to 2.0×10^{3} μm, including 13 UV through visible points, which are included for the grain heating. The grid includes the 30 photometric data points from Campbell et al. (1995), which are presented in Table 5. Double points have been shifted by the smallest possible fraction, e.g. the four 800 μm points are included in the grid as: 8.001d 02 8.000d 02 7.999d 02 7.998d 02.
(*WLAMBDA =*

```
2.000d 03 1.300d 03 1.100d 03 1.099d 03 8.001d 02 8.000d 02 7.999d 02
7.998d 02 4.500d 02 4.499d 02 4.000d 02 3.999d 02 3.500d 02 3.000d 02
2.350d 02 2.000d 02 1.600d 02 1.200d 02 1.000d 02 9.500d 01 9.499d 01
9.000d 01 8.000d 01 7.000d 01 6.000d 01 5.000d 01 4.700d 01 4.000d 01
3.300d 01 3.000d 01 2.500d 01 2.000d 01 1.999d 01 1.800d 01 1.300d 01
1.100d 01 1.000d 01 9.999d 00 8.000d 00 6.000d 00 4.800d 00 4.000d 00
3.500d 00 3.000d 00 2.200d 00 1.800d 00 9.000d-01 7.000d-01 5.500d-01
4.350d-01 3.460d-01 2.750d-01 2.500d-01 2.150d-01 2.000d-01 1.800d-01
1.430d-01 1.300d-01 1.000d-01 9.100d-02)
```

INDEX FOR REFERENCE WAVELENGTH TO OPTICAL DEPTH
The reference wavelength for which the optical depth is specified is 95 μm point, the 20^{th} point on the grid. (*IOF = 20*)

INCIDENT FLUX AT OUTER BOUNDARY
The incident flux at the outer boundary at each wavelength is determined by linear interpolation of the interstellar radiation field taken from the test input file on the wavelength grid, see section 2.1.4. The inputs are intensities, CSDUST3 internally converts them into fluxes.
(*FLUXSD =*

```
3.680d-01 2.638d-01 2.571d-01 2.503d-01 2.571d-01 2.165d-01 1.894d-01
1.894d-01 2.368d-01 1.894d-01 6.629d-01 4.735d-01 2.029d-01 1.353d-04
1.353d-04 1.353d-04 1.353d-04 1.353d-04 4.059d-01 4.059d-01 3.788d-01
1.353d-04 1.353d-04 1.353d-04 1.353d-04 4.059d-01 2.976d-01 1.353d-04
1.826d-01 4.059d-01 1.826d-01 1.826d-01 1.353d-01 1.353d-04 1.015d-01
1.353d-04 1.015d-01 1.353d-01 1.015d-01 1.353d-04 1.353d-01 1.353d-04
1.353d-01 1.353d-04 1.353d-01 1.353d-04 1.353d-04 1.353d-04 1.353d-04
1.353d-04 1.353d-04 1.353d-04 1.353d-04 1.353d-04 1.353d-04 1.353d-04
1.353d-04 1.353d-04 1.353d-04 1.353d-04)
```

NUMBER OF GRAIN TYPES/MODELS
One grain model that, which is already based on a mixture of grain types, from Draine & Li is used, see section 3.2.
(*IMIX = 1*)

NAME OF GRAIN CORE COMPOSITION
The 8-character name DRAINLI is used to identify the grain model from Draine & Li.
(*GRAINC(1) = DRAINLI*)

GRAIN CORE RADIUS
The grain core radius is set to 5.0×10^{-1} μm, which is a characteristic value for the grain size. The grain core radius has no effect on the model since it is the weighted absorption and scattering cross-section that are inputted to CSDUST3.
(*AC(1) = 5.000D-01*)

NAME OF GRAIN MANTLE COMPOSITION
A grain model is inputted and not a grain type. The model already deals with different grain size distributions and grain compositions, therefore the 8-character name is set to

NOMANTLE because no mantle needs to be specified.
(*GRAINM(1) = NOMANTLE*)

GRAIN MANTLE RADIUS
No grain mantle present gives for the radius 0 μm.
(*AM(1) = 0.000D 00*)

ABUNDANCE TYPE
For the dust abundance distribution a uniform distribution or a distribution read from the input file can be chosen. It doesn't matter here since there is a grain model. The parameter is set on reading the abundance distribution from the input file.
(*IREADA = 1*)

DUST PROPERTIES
As discussed in section 3.2 the dust properties are determined by linear interpolation of the dust model from Draine & Li on the wavelength grid. For easy reading the wavelength is shown as a DUMMY variable in the input file. The values for the scattering coefficient and the absorption coefficient are given 'per hydrogen nucleon'.
(*QABSI(NFD, N) = / QSCAI(NFD, N) = / GBARI(NFD, N) = / DUMMY = *)

```
2.176d-27 0.000d 00-2.558d-03 2.000d 03          9.322d-24 2.797d-27-2.412d-02 2.500d 01
4.483d-27 0.000d 00-3.800d-03 1.300d 03          1.435d-23 7.177d-27-2.384d-02 2.000d 01
5.932d-27 0.000d 00-4.200d-03 1.100d 03          1.437d-23 7.185d-27-2.383d-02 1.999d 01
5.941d-27 0.000d 00-4.200d-03 1.099d 03          1.617d-23 1.116d-26-2.509d-02 1.800d 01
1.013d-26 0.000d 00-4.800d-03 8.001d 02          1.341d-23 4.023d-26-2.870d-02 1.300d 01
1.014d-26 0.000d 00-4.800d-03 8.000d 02          2.831d-23 8.209d-26-3.094d-02 1.100d 01
1.014d-26 0.000d 00-4.800d-03 7.999d 02          4.073d-23 1.222d-25-3.440d-02 1.000d 01
1.014d-26 0.000d 00-4.800d-03 7.998d 02          4.074d-23 1.222d-25-3.440d-02 9.999d 00
2.842d-26 0.000d 00-5.300d-03 4.500d 02          1.528d-23 2.477d-25-5.035d-02 8.000d 00
2.844d-26 0.000d 00-5.300d-03 4.499d 02          9.341d-24 8.022d-25-5.283d-02 6.000d 00
3.582d-26 0.000d 00-5.200d-03 4.000d 02          1.185d-23 1.874d-24-4.245d-02 4.800d 00
3.584d-26 0.000d 00-5.200d-03 3.999d 02          1.582d-23 3.530d-24-2.194d-02 4.000d 00
4.703d-26 0.000d 00-5.162d-03 3.500d 02          1.967d-23 5.376d-24 1.895d-03 3.500d 00
6.522d-26 0.000d 00-4.900d-03 3.000d 02          2.528d-23 8.355d-24 3.937d-02 3.000d 00
1.110d-25 0.000d 00-4.343d-03 2.350d 02          4.133d-23 1.792d-23 1.293d-01 2.200d 00
1.541d-25 0.000d 00-3.700d-03 2.000d 02          5.588d-23 2.737d-23 1.837d-01 1.800d 00
2.450d-25 0.000d 00-2.067d-03 1.600d 02          1.516d-22 9.572d-23 3.980d-01 9.000d-01
4.416d-25 0.000d 00 2.529d-03 1.200d 02          2.173d-22 1.435d-22 4.782d-01 7.000d-01
6.425d-25 0.000d 00 7.100d-03 1.000d 02          3.053d-22 2.029d-22 5.403d-01 5.500d-01
7.164d-25 0.000d 00 8.091d-03 9.500d 01          4.173d-22 2.688d-22 5.734d-01 4.350d-01
7.166d-25 0.000d 00 8.093d-03 9.499d 01          5.458d-22 3.307d-22 5.780d-01 3.460d-01
8.040d-25 0.000d 00 9.031d-03 9.000d 01          6.946d-22 3.922d-22 5.575d-01 2.750d-01
1.036d-24 0.000d 00 9.900d-03 8.000d 01          8.196d-22 4.306d-22 5.506d-01 2.500d-01
1.382d-24 0.000d 00 7.210d-03 7.000d 01          1.171d-21 4.920d-22 5.624d-01 2.150d-01
1.919d-24 1.919d-28-1.229d-04 6.000d 01          1.026d-21 4.607d-22 5.832d-01 2.000d-01
2.786d-24 2.786d-28-1.142d-02 5.000d 01          9.017d-22 4.087d-22 6.204d-01 1.800d-01
3.141d-24 3.141d-28-1.443d-02 4.700d 01          1.059d-21 3.833d-22 6.772d-01 1.430d-01
4.244d-24 4.244d-28-1.912d-02 4.000d 01          1.182d-21 4.054d-22 6.824d-01 1.300d-01
5.834d-24 1.167d-27-2.286d-02 3.300d 01          1.796d-21 4.851d-22 6.518d-01 1.000d-01
6.830d-24 1.366d-27-2.390d-02 3.000d 01          2.024d-21 4.943d-22 6.644d-01 9.100d-02)
```

⇓

FRACTIONAL ABUNDANCE OF GRAIN TYPE
Since one grain type/model is used here, the fractional abundance is set to 1.
(*ABUNDI(1) = 1.000D 00*)

INITIAL DUST TEMPERATURE
A guess for the initial dust temperature can be calculated or read from the data file. Here is chosen to calculate the initial guess for the dust temperature, although reading a guess for the initial dust temperature from the input file could result in faster convergence, when the initial dust temperature is guessed correctly.
(*IREADT = 0*)

ESTIMATED DUST TEMPERATURE AT OUTER BOUNDARY
Although not read into CSDUST3, see previous parameter, the dust temperature at the outer boundary is estimated to be 10 Kelvin, which is approximately the temperature of the cold interstellar medium. (*TDS = 1.000D 01*)

ESTIMATED DUST TEMPERATURE AT INNER BOUNDARY
Although also not read into the program, see previous two parameters, the dust temperature at the inner boundary is estimated at 1000 Kelvin (*TDC = 1.000D 03*)

OPTICAL DEPTH AT REFERENCE WAVELENGTH
The optical depth at 95 μm is set to 0.30 (see Table 4).

(*TAU0F = 0.300D 00*)

POWER LAW INDEX
The power law index is set to 1 (see Table 4). However, after running the model probably a numerical problem occurred (in the matrix inversion). This problem was solved by setting the power law index to 9.999×10^{-1}, which is according to us close enough to 1.
(*RHOCS = 9.999D-01*)

EFFECTIVE TEMPERATURE CENTRAL HEAT SOURCE
The effective temperature central heat source is set to 25,000 Kelvin.(see Table 4).
(*TSTAR = 2.500D 04*)

EFFECTIVE LUMINOSITY CENTRAL HEAT SOURCE
The effective luminosity central heat source is set to 250,000 $L_{\odot}$ (see Table 4).
(*TLUM = 2.500D 05*)

BEAM CONVOLUTION
There is the choice to do a beam convolution. There is chosen to do the beam convolution, because then a direct comparison with the data presented by Campbell et al. (1995) can be made.
(*ICONV = 1*)

BEAM WIDTHS OF BEAM PATTERN (NOT FWHM!)
To do the convolution the half beam widths, given as fraction of the radius (see section 2.1.7), need to be provided. Wavelengths that don't belong to the 30 photometric data points provided by Campbell et al. (1995) are given an half beam width of 1″.

```
3.680d-01 1.353d-04 2.638d-01 1.353d-04 2.571d-01 1.353d-04 2.503d-01
1.353d-04 2.571d-01 1.353d-04 2.165d-01 1.353d-04 1.894d-01 1.353d-04
1.894d-01 1.353d-04 2.368d-01 1.353d-04 1.894d-01 1.353d-04 6.629d-01
1.353d-04 4.735d-01 1.353d-04 2.029d-01 1.353d-04 4.059d-01 4.059d-01
4.059d-01 4.059d-01 3.788d-01 1.353d-04 4.059d-01 4.059d-01 2.976d-01
1.353d-04 1.826d-01 1.353d-04 4.059d-01 4.059d-01 1.826d-01 1.353d-04
1.826d-01 1.353d-04 1.353d-01 1.015d-01 1.015d-01 1.353d-04 1.015d-01
1.353d-04 1.353d-01 1.015d-01 1.015d-01 1.353d-04 1.353d-01 1.015d-01
1.353d-01 1.015d-01 1.353d-01 1.015d-01
```

The selected inputs are written into a file, which is presented in Appendix D. The file is run with CSDUST3. The results are presented in the next section.

4 Results

Computations were done on a 2 GHz computer running Red Hat Linux 7.2. 33 iterations were needed for convergence. The output that is used for closer investigation are the Spectral Energy Distribution (SED), the density- and temperature structure ($n(r)$, $T(r)$) and the 95μm and 800μm maps. Output from the program is in cgs units.

4.1 Spectral Energy Distribution

For the calculation of the Spectral Energy Distribution (SED) the convolved intensities and the beam widths are needed. The convolved intensities are located at the CONVOLVED INTENSITIES, AT GIVEN X AND Y FROM CLOUD CENTER section in the output file, see for example Appendix C.2 line 9995. The first column is a reference index, the second column is the wavelength in μm, the third column are the Gaussian beam widths (σ) and the fourth through the last column are the different X positions. The SED is made through the core, so Y = X = 0 is used.

The data on the 30 photometric data points are manually extracted from the output file; the added UV through visible wavelength points and the intermediate wavelength points are taken out of the dataset. The 30 photometric data points are presented in Table 6. For

comparison the observed data points and the difference between model and observation are also shown. CSDUST3 presents the intensity in erg·s^{-1}·cm^{-2}·Hz^{-1}·sr^{-1}, to make a

Wavelength (μm)	Model Flux (Jy)	Beam ($''$)	Observed Flux (Uncertainty) (Jy)	Difference (Jy)
2.000e+03	8.851	27.2	4.400 (0.440)	4.45
1.300e+03	5.768	19.5	5.500 (0.320)	0.27
1.100e+03	7.341	19.0	2.750 (0.400)	4.59
1.099e+03	7.032	18.5	6.800 (0.460)	0.23
8.001e+02	16.197	19.0	13.500 (2.700)	2.70
8.000e+02	12.284	16.0	17.000 (1.300)	-4.72
7.999e+02	9.749	14.0	15.000 (1.100)	-5.25
7.998e+02	9.754	14.0	13.900 (0.300)	-4.15
4.500e+02	99.977	17.5	112.000 (3.400)	-12.02
4.499e+02	68.682	14.0	81.000 (2.000)	-12.32
4.000e+02	451.686	49.0	500.000 (125.000)	-48.31
3.999e+02	357.176	35.0	250.000 (100.000)	107.18
3.500e+02	192.078	15.0	200.000 (100.000)	-7.92
1.000e+02	15946.214	30.0	15000.000 (4500.000)	946.21
9.500e+01	17108.510	30.0	16900.000 (5100.000)	208.51
9.499e+01	15235.342	28.0	15000.000 (4600.000)	235.34
5.000e+01	13930.769	30.0	14000.000 (4200.000)	-69.23
4.700e+01	8427.310	22.0	9800.000 (2900.000)	-1372.69
3.300e+01	1190.412	13.5	2860.000 (165.000)	-1669.59
3.000e+01	1318.546	30.0	8200.000 (2460.000)	-6881.45
2.500e+01	151.458	13.5	1290.000 (260.000)	-1138.54
2.000e+01	10.094	13.5	719.000 (143.000)	-708.91
1.999e+01	8.020	10.0	427.000 (80.000)	-418.98
1.300e+01	1.475	7.5	450.000 (225.000)	-448.53
1.000e+01	0.000	7.5	6.600 (3.300)	-6.60
9.999e+00	0.000	10.0	112.000 (19.000)	-112.00
8.000e+00	0.033	7.5	213.000 (100.000)	-212.97
4.800e+00	0.001	10.0	54.000 (5.000)	-54.00
3.500e+00	0.000	10.0	5.400 (0.900)	-5.40
2.200e+00	0.000	10.0	0.010 (0.004)	-0.01

Table 6: Convolved photometric data points. The data is extracted from CSDUST3 and it is for a scan through the core. The results are needed to calculate the SED.

comparison with the results from Campbell et al. (1995) the quantity is rewritten into a flux in Jy / BEAM. The conversion factor between Jansky and erg·s^{-1}·cm^{-2}·Hz^{-1} is a factor 10^{23}. To get a flux, the intensities are multiplied by the area of the beams: $2\pi\sigma^2$, where σ is the width of the beam in radians. When using the FWHM beam widths given in $''$ a conversion to sr is needed as also the conversion from FWHM to σ. The conversion factor to go from $^{\square}''$ to sr^{-1} is $2.35{\cdot}10^{-11}$. The conversion from FWHM to σ is $(8\ln 2)^{-\frac{1}{2}}$. All in all the needed conversions result in

$$\text{FLUX/BEAM } [\text{erg}\cdot\text{s}^{-1}\cdot\text{cm}^{-2}\cdot\text{Hz}^{-1}\cdot\text{sr}^{-1}] = \text{INTENSITY} \times 1\cdot 10^{23} \times 2\pi \frac{2.25\cdot 10^{-11} \times \text{FWHM}[''] }{\sqrt{8\ln 2}} [\text{Jy/BEAM}]$$

The resulting SED is shown in Fig. 11 and is the main result of this exercise. When you want to speak about the the fit of the modeled SED to the observed SED, the reduced χ^2 can be calculated according to $\chi^2 = \frac{1}{N}\sum_{i=1}^{N}\left(\frac{d_i - m_i}{\sigma_i}\right)^2$. Since it seems that the fit in the sub mm part is better, an overall fit and a fit in the sub mm part should be made. This is not done here.

4.2 Density and Temperature Structure

The output of CSDUST3 include the density and temperature profiles as function of fractional radial size. They are located in the output file almost at the end, see for example

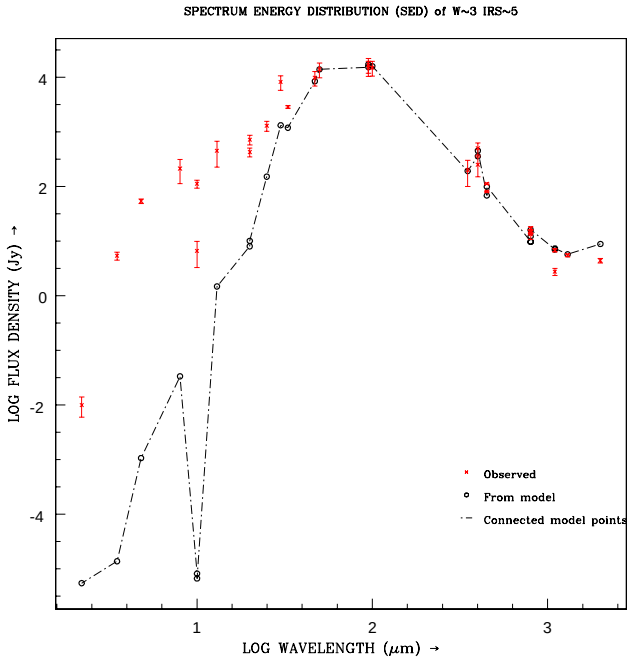

Figure 11: Spectral Energy Distribution (SED) calculated from data extracted from CSDUST3, the main result of this exercise.

Appendix C.2 line 10616. The third column presents the radial fraction (R), the fourth column (RHOD) presents the dust number density and the sixth column (TD) presents the dust temperature in K.

The fractional radial scale can be rewritten into a displacement from the center in arc seconds (α) with the use of the relation

$$\alpha = \frac{\arctan(X)}{D} \cdot 3600 \tag{4.1}$$

where X is the fractional radial scale, R is the radial size of the cloud and D is the distance to the cloud. This all results into

$$0.35 \text{ pc} \equiv 31.39'' \equiv 1 \text{ (in units of } \frac{r}{R})$$

The dust number density distribution is actually a Hydrogen number density because the input of the dust characteristics was 'per hydrogen nucleon'. The hydrogen number density distribution together with the temperature distribution are shown in Fig. 12. The tabulated values can be found in Table 12 in Appendix E. From the hydrogen number density distribution the total mass of the cloud can be estimated. The total number of hydrogen nucleons is given by

$$N_{\rm H} = \int_{r_{\rm c}}^{R} 4\pi n_{\rm H}(r) r^2 {\rm d}r$$

Multiplying the number of hydrogens nucleons with the hydrogen mass results into the total mass in hydrogen which is about the total mass of the cloud.

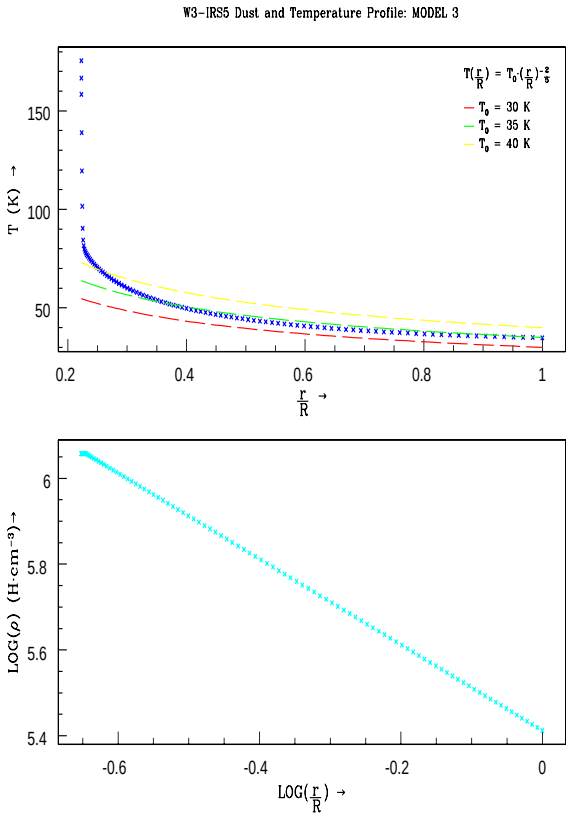

Figure 12: Top: resulting temperature profile with different fits for T_0 with $T(\frac{r}{R}) = T_0 \cdot (\frac{r}{R})^{-\frac{2}{5}}$ Bottom: resulting hydrogen Number Density profile which clearly shows the power law index γ of 1.

The integration can be done numerically, but since here the dust distribution is a power law, with power law index γ, the total mass can also be found analytically.
The power law is given by $n_{\mathrm{H}}(x) = n_{\mathrm{H0}} x^{-\gamma}$, with $x = \frac{r}{R}$, equating this into the integral and integrating from r_{c} to R results into

$$N_{\mathrm{H}} = \int_{x_{\mathrm{c}}}^{X} n_{\mathrm{H0}} x^{-\gamma} 4\pi R^2 x^2 R \mathrm{d}x = 4\pi n_{\mathrm{H0}} R^3 \int_{x_0}^{X} x^{2-\gamma} \mathrm{d}x = \frac{4\pi n_{\mathrm{H0}} R^3}{3-\gamma} \left[x^{3-\gamma} \right]_{x_0}^{X}$$

Taking the power law index γ as 1 and determining $n_{\mathrm{H}\ 0}$ from a single point, the total mass can be estimated. Taking for example (1.000e+00[x]; 2.584e+05) from Table 12 in Appendix E it follows that $n_{\mathrm{H0}} = 2.584 \cdot 10^5\ \frac{\mathrm{H}}{\mathrm{cm}^3}$. Now solving for N_{H} gives

$$N_{\mathrm{H}} = 2\pi \cdot 2.584\mathrm{e}+05 \cdot (0.35 \cdot 3.084 \cdot 10^{18})^3 \cdot 0.95 = 9.70 \cdot 10^{59} \text{ hydrogen nucleons}$$

Multiplying N with the hydrogen mass of $1.7 \cdot 10^{-27}$ kg results into the total mass in hydrogen M_{H}

$$M_{\mathrm{H}} = 9.70 \cdot 10^{59} \cdot 1.7 \cdot 10^{-27} = 1.65 \cdot 10^{33} \text{ kg} = 825\ M_{\odot}$$

Taking the gas to dust mass ratio from Draine & Lee (1984) of 100 gives for the conversion factor from 'per grain' to 'per hydrogen nucleon'

$$100 = \frac{M\text{gas}}{M_{\text{dust}}} = \frac{m_{\text{H}}}{\frac{4}{3}\pi\bar{\rho}\bar{r}^3} \cdot \frac{N_{\text{H}}}{N_{\text{dust}}} \Longrightarrow \frac{N_{\text{H}}}{N_{\text{dust}}} = 7.42 \cdot 10^{11}$$

where $\bar{\rho}$ and $\bar{r}$ are the average grain density respectively the average grain radius. Values are given in Table 7.

$\bar{\rho}$	3 g·cm^{-3}
$\bar{r}$	0.1 μm
$\frac{\text{gas}}{\text{dust}}$	100

Table 7: Average grain characteristics, values adopted from Hildebrand (1983).

4.3 95 μm and 800 μm Maps

For the construction of the intensity maps the convolved intensities are needed. The convolved intensities are again located at CONVOLVED INTENSITIES, AT GIVEN X AND Y FROM CLOUD CENTER section in the output file, see for example Appendix C.2 line 9995. The convolved intensities are presented for each wavelength on a 10 by 10 grid (X, Y). In the input file the first column is a reference index, the second column is the wavelength in μm, the third column are the Gaussian beam widths (σ) and the fourth through the last column are the different intensities at a specified Y for the different X positions.

For all sixty wavelength points the 100 (10 by 10) grid points (= 6000 points) are read in a data cube by BuI. BuI creates a postscript file containing all 60 contour maps. The 95 μm and 800 μm maps are extracted by hand. The 95 μm map is shown in Fig. 14 and the 800 μm map is shown in Fig. 13.

5 Discussion

The discussion will not be on the explanation of the results and how the agreement with observed data is, but about the differences with the results from Campbell et al. (1995).A discussion on the explanation and interpretation of the results can be found in the paper from Campbell et al. (1995). A look will also be taken into what can be done with the acquired results for the temperature structure and the density structure.

First the SED. It's unfortunate that Campbell et al. (1995) do not present their values for the calculated SED derived from their model 3. In this way no direct comparison can be made. A comparison is based on their Fig. 16, Campbell et al. (1995) and is shown here in Fig. 8, and Fig. 11.
At first glance the overall shape of Fig. 11 seems not to differ to much from that of Fig. 8. A closer comparison between Fig. 8 and Fig. 11 shows that in Fig. 8 points below a LOG FLUX DENSITY / BEAM of -4 are dropped. In both figures the radio fit seems to

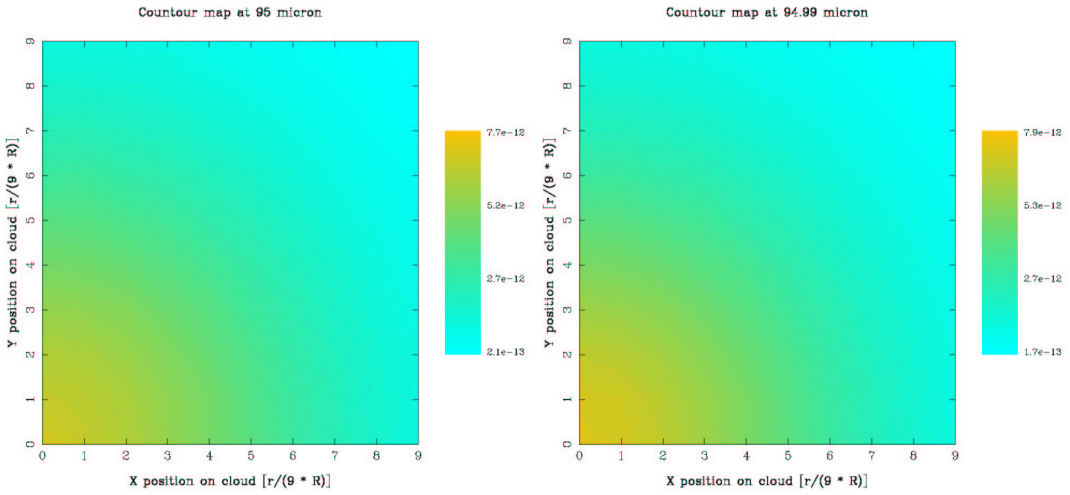

Figure 13: The two 95 μm maps. Intensities are given in erg·s^{-1}· cm^{-2}·Hz^{-1}·sr^{-1}. Left: 28″ beam. Right: 30″ beam.

be better than the that of the shorter wavelengths. Both figures also display the silicate feature at 10 μm and the feature at 800 μm. The striking difference is that in Fig. 11 the silicate absorption feature is much deeper than that in Fig. 8 and that in Fig. 11 the flux at 1100 μm rises again and in Fig. 8 it keeps dropping off.

Second the temperature and number density distribution. Campbell et al. (1995) do not make use of the temperature and density structure outputted by CSDUST3 so using it as a test is not possible. However, in view of the goal of this research in finding the temperature and density structure and standardizing the method in doing this, the density profile has been checked by estimating the total mass and comparing this to the virial mass found by van der Tak et al. (2000), although they used a different γ for the power law index for the number density distribution. The virial mass found by van der Tak et al. (2000) is 355 $M_\odot$, compared to the 825 $M_\odot$ found here it seems to be of the right order.
For optically thin dust the relation $T = T_0\left(\frac{r}{R_0}\right)^{-\frac{2}{5}}$ is expected. Plotted in the Top of Fig. 12 are three fits to the relation. If it is assumed that the green curve is the best fit, it shows when the cloud becomes optically thick and also the outer cloud temperature. Comparing the outer cloud temperature with that calculated by van der Tak et al. (2000) of 33 K it seems to be in quite good agreement.
Further the dust temperature can be used to indicate if an assumption of evaporated grain mantles is valid or not. Also when calculating the grain temperature the brightness temperature (T_B) at each wavelength is given, which can be used for further modeling.

Finally the 95 μm and 800 μm maps. Since here we deal with spherical geometry a radial scan could also suffice. When dealing with other geometries then spherical, a map would be sure insightful. However making the maps for the first time showed clearly that there had been made a mistake in the calculations of the beam widths. After making the corrections to the beam widths and re-running the model the maps were what was expected; maps with circular patterns. Further justification for the maps is that it completes the list of what can be done with the data extracted from CSDUST3. No radial scan was

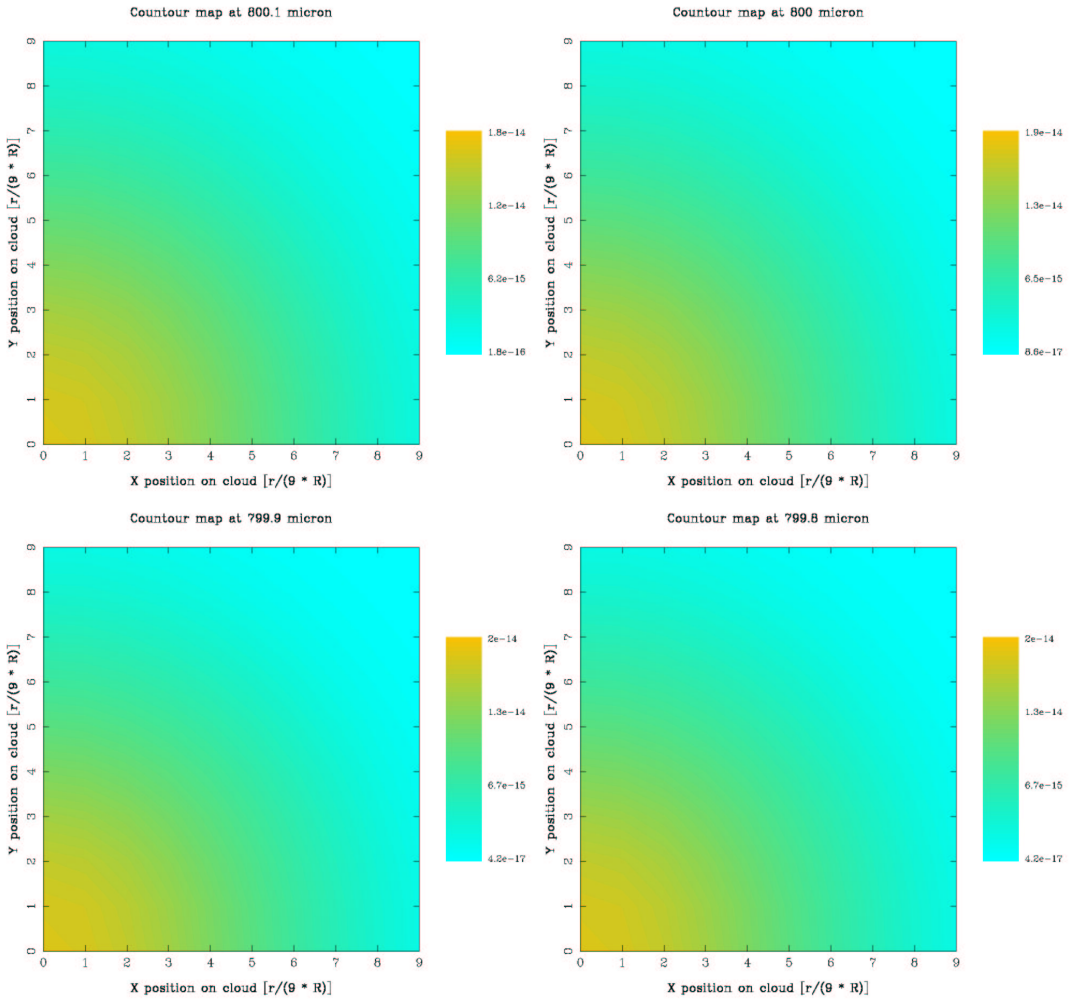

Figure 14: The four 800 μm maps. Intensities are given in erg·s^{-1}· cm^{-2}·Hz^{-1}·sr^{-1}. Top left: 14″ beam. Top right: 14″ beam. Bottom left: 16″ beam. Top-right: 19″ beam.

made, however this would be useful in making a comparison with the radial scan profiles presented by Campbell et al. (1995) and providing yet another test for the procedure.

6 Summary and Conclusions

The goal of this research was to standardize the method in determining the temperature and density structure for a arbitrary high mass star formation region. To test the method reproduction of the Spectral Energy Distribution (SED) from Campbell et al. (1995) was used. The SED was on W 3 IRS 5, a dense high mass star formation region located in the Perseus arm located at approximately the distance of 2.3 kpc.
The determination of the temperature and density structure is done by the computer program CSDUST3 from Egan et al. (1988) implementing the model for radiative transfer from Leung (1975, 1976b). Because CSDUST3 uses quite extensive and 'unreadable' input and output files (over 10,000 lines!) an user interface program, BuI (Boersma user Interface) has been written to overcome this. BuI can also create direct graphical representations of

some parameters. It should be remarked that the use of the 99% level fit to the inner gaussian and the powerlaw instead of the 80% fit version of CSDUST3 hadn't had any effect in this case. This was due to the inner cavity since no singularity at the center was created this way. The procedure has become answering the questions which input parameters to give to CSDUST3. In section 3.4 an extended overview of the input parameters is given and determining them is all that is needed to solve the problem of finding the density and temperature structure. BuI can provide direct graphical representation of the two profiles.

Although there were some small discrepancies in the SED produced by Campbell et al. (1995) and the SED produced here, there seems to be enough agreement between the two SEDs to say that the method is successful. Also the agreement of the found total mass and outer cloud temperature of IRS 5 with that found by van der Tak et al. (2000) suggest that the method was successful. The small discrepancies that do exist are thought to originate from the use of a different dust model, that from Draine & Li instead of that from Draine & Lee, or that they come from the uncertainty in the spatial and wavelength grid that is used by Campbell et al. (1995). Since IRS 5 is embedded in W 3 the use of the normal external radiation field is questionable and it is not sure whether Campbell et al. (1995) use it and it would also explain why in our case the flux rises again beyond 1100 μm. At those wavelengths the Cosmic Microwave Background provides additional flux. As also mentioned in the presentation on the data for the external radiation field, the radiation field taken from the trial input file itself gives rise to questions. Taking a look at Fig. 10 shows directly that it is hard to find the three assumed blackbody curves. On the eye the three maximums could be located at approximately 1.60μm , 160 μm and 2000 μm, which respectively corresponds to blackbody temperatures of 1811 K, 18.11K and 1.45 K. The last temperature is impossible since nothing can be colder than the Cosmic Microwave Background Temperature of 2.8 K. Moreover are the three points located around 0.6 μm, the three points located around 250 μm and the single point located at about 4000 μm very strange since the do not seem to lie on a blackbody curve. Recommend is to use, when needed, the external radiation field provided by Mathis et al. (1983) which is shown in Fig. 3 in section 2.1.4.

There are a few remaining questions and possible additions to this research. The most important still standing question is if when using the Draine & Lee dust model instead of that from Draine & Li the discrepancies with Campbell et al. (1995) are less. Further questions that could be important for using the model is the influence of using different geometries. Since in this research a spherical geometry is assumed, in accordance with Campbell et al. (1995), problems stemming from different geometries are not looked at. So additions to the research could be researching different geometries.
To make more use of the results on IRS 5 produced by Campbell et al. (1995) radial profiles from the 800 μm and a 95 μm maps through the core could be made for an additional measure of the correctness of the procedure. Also reproducing the models 1, 2 and 4 from Campbell et al. (1995) can be a extra measure. A measure not from Campbell et al. (1995) is the reproduction of results from van der Tak et al. (1999) which uses different grain models such as Ossenkopf and Henning, Li and Greenberg and Mathis et al. To check the overall stability of the routines, changes of the input parameters, such as e.g. changing the power law, the beam sizes and the spatial and wavelength grid should be investigated. A task still to be completed is adding more routines to BuI such that manually handling the input and output files is not needed at all anymore.

References

Burden, R. L. & Faires, J. D. 2001 (Rooks & Cole)

Campbell, M. F., Butner, H. M., Harvey, P. M., Evans, N. J., Campbell, M. B., & Sabbey, C. N. 1995, ApJ, 454, 831

Claussen, M. J., Gaume, R. A., Johnston, K. J., & Wilson, T. L. 1994, ApJ Lett., 424, L41

Draine, B. T. & Lee, H. M. 1984, ApJ, 285, 89

Egan, M. P., Leung, C. M., & Spanga, J. F. J. 1988, Comput. Phys. Commun.

Hildebrand, R. H. 1983, QJRAS, 24, 267

Leung, C. M. 1975, ApJ, 199, 340

—. 1976a, J. Quant. Spectrosc. Radiat. Transfer

—. 1976b, ApJ, 209, 75

Mathis, J. S., Mezger, P. G., & Panagia, N. 1983, A&A, 128, 212

Ribicky & Lightman. 1985 (John Wiley & Sons Inc.)

Rutten, R. J. 1995 (Sterrekundig Insituut Utrecht)

van der Tak, F. F. S., van Dishoeck, E. F., Evans, N. J., Bakker, E. J., & Blake, G. A. 1999, ApJ, 522, 991

van der Tak, F. F. S., van Dishoeck, E. F., Evans, N. J., & Blake, G. A. 2000, ApJ, 537, 283

Appendices

A Meaning of symbols in equations

A.1 Equation (2.1)

Variable	Meaning
$\mu \equiv \cos(\theta)$	Scattering angle
θ	Angle between the outward normal and the direction of photon propagation at r
r	Radial distance
$I_\nu(r,\mu)$	Intensity at (r,μ)
ν	Frequency in Hz
$m \equiv \begin{cases} 0 & \text{planar} \\ 1 & \text{spherical} \end{cases}$	geometry parameter
$\sigma_\nu^a(r)$	Absorption coefficient in V^{-3}
$B_\nu(r) = B_\nu = \frac{1}{e^{\frac{h\nu}{kT}}-1}$	Planck Function
h	Planck constant
k	Boltzmann constant
T	Temperature in Kelvin
$\sigma_\nu^s(r)$	Scattering coefficient in V^{-3}
$p_\nu(\mu,\mu')$	Normalized phase function; probability of scattering from direction μ' into μ

Table 8: Meaning of symbols in equation (2.1)

With normalization of the phase function; $\frac{1}{2}\int_{-1}^{+1} p_\nu(\mu-\mu')\mathrm{d}(\mu-\mu 1) = 1$ is meant.

A.2 Equation (2.4), (2.5) and (2.6)

Variable	Meaning
$\kappa_\nu^* \equiv \sigma_\nu^a$	Absorption coefficient in V^{-3}
$\epsilon_\nu^* \equiv \sigma_\nu^a B_\nu$	Emissivity
r	Radial parameter
r_c	Core radius

Table 9: Meaning to symbols in equation (2.4), (2.5) and (2.6)

B Input parameters and their meaning

B.1 Parameters and their meaning

Variable	Meaning	Line
NMODEL	Number of models to run	1
IGEOM	Geometry; 0 = slab, 1 = cylindrical, 2 = spherical	2
IEMERG	IGEOM = 1; emergent intensities for: 1 = 4 angles, 0 = 1 angle	
IEDFTR	Use Eddington-Approximation: 0 = yes, 1 = no	3
IOUT	Output: 0 = 'normal' printout, 1 = detailed printout	3
IC	Central core: 0 = no, 1 = yes	
NH	Use total net flux at core: 0 = no, 1 = yes	
ISCA	Use first order scattering: 1 = yes, 0 = no	
IB	Incident flux at outer boundary: 0 = yes, 1 = no	
IDIST	Dust distribution: 0 = power law, 1 = Gaussian	
AJ0	Normalization constant for J*	4
EPS	Maximum fractional error allowed for convergence	
ITMAX	Maximum number of iterations	4
R(NR)	Radial grid (100 points) $\frac{r}{R}$	5 - 19
NFD	Number of wavelength grid points	20
IOF	Index for reference wavelength to optical depth	20
WLAMBDA	Wavelength grid in μ	21 - 29
FLUXSD(NFD)	Incident flux at outer boundary R $[H^-(R)]$	30 - 38
IMIX	Number of grain type (max = 5)	39
GRAINC(1)	Grain core composition (8 character name)	40
AC(1)	Grain core radius in μ	
GRAINM(1)	Grain mantle composition (8 character name)	
AM(1)	Grain mantle radius in μ	
IREADA	0 = uniform abundance, 1 = read abundance from datafile	
QABSI(NFD, N)	$Q_{\text{absorption}}\pi a^2$ at wavelength (in μ) for grain type N	41 - 99
QSCAI(NFD, N)	$Q_{\text{scattering}}\pi a^2$ at wavelength (in μ) for grain type N	
GBARI(NFD, N)	Scattering asymmetry parameter g for grain type ($0 \leq g \leq 1$)	
DUMMY	Corresponding wavelength, for reference only	
ABUNDI(N)	Fractional abundance of grain type N at each spatial grid point	100
IREADT	Initial dust temperatures: 0 = guess from data, 1 = calculate	101
TDS	Estimated dust temperature at outer boundary in Kelvin	
TDC	Estimated dust temperature at inner boundary in Kelvin	
RMAX	Outer cloud radius in parsecs	163
TAU0F	Total optical depth to cloud center for IOF wavelength	
RHOCS	Power law index (IDIST = 0) or $\frac{n_{\text{central}}}{n_{\text{surface}}}$ (IDIST = 1)	
TSTAR	Effective Temperature central heat source for $\lambda > 912$ Å in Kelvin	
TLUM	Effective Luminosity central heat source for $\lambda > 912$ Å in $L_\odot$	
ICONV	Beam convolution: 0 = no, 1 = yes	164
SIGMA(NFD)	Half width of Gaussian beam pattern at each wavelength	165

Table 10: Input parameters and their meaning, for an example input file see Appendix B.2, line numbers refer to this file

B.2 Example input file

An example of an input file, see table 10 in Appendix B.1 for the meaning of the parameters.

```
NMODEL=  1                                                                  1
 IGEOM=2 IEMRG=0                                                            2
IEDFTR=1  IOUT=1    IC=1    NH=1  ISCA=1    IB=1 IDIST=1                   3
 1.000D-30 1.000D-03  20                                                    4
 1.500d-01 1.505d-01 1.510d-01 1.515d-01 1.520d-01 1.530d-01 1.540d-01      5
 1.550d-01 1.560d-01 1.570d-01 1.580d-01 1.590d-01 1.600d-01 1.700d-01      6
 .
 .
 .
 9.500d-01 9.600d-01 9.700d-01 9.800d-01 9.900d-01 9.950d-01 9.970d-01      18
 9.990d-01 1.0000d+00                                                       19

   59   37                                                                  20
 5.000d 03 4.000d 03 3.000d 03 2.000d 03 1.000d 03 8.000d 02 6.000d 02      21
 4.500d 02 4.000d 02 3.000d 02 2.350d 02 2.000d 02 1.900d 02 1.800d 02      22
 .
 .
 .
 2.300d-01 2.150d-01 2.100d-01 2.000d-01 1.800d-01 1.430d-01 1.300d-01      28
 1.100d-01 1.000d-01 9.100d-02                                              29

 1.771d-15 5.938d-16 3.238d-15 4.120d-15 2.347d-15 1.264d-15 3.572d-16      30
 1.460d-17 7.065d-18 1.713d-17 6.290d-18 2.976d-17 7.990d-18 8.530d-18      31
 .
 .
 .
 1.445d-20 1.423d-20 1.405d-20 1.375d-20 1.333d-20 1.230d-20 1.143d-20      37
 8.175d-21 4.850d-21 2.950d-21                                              38

    2                                                                       39
GRAPHITE  5.000D-01 NOMANTLE  0.0  0                                        40
 1.070d-18 0.000d 00 0.000d 00 5.000d 03                                    41
 .
 .
 .
 1.030d-11 0.000d 00 0.000d 00 9.100d-02                                    99
 5.000D-01                                                                  100
SILICATE  5.000D-01 NOMANTLE  0.0  0                                        101
 1.070d-17 0.000d 00 0.000d 00 5.000d 03                                    102
 .
 .
 .
 1.430d-11 9.150d-12 5.500d-02 9.100d-02                                    160
 5.000D-01                                                                  161

    0      4.000D 02 1.500D 03                                              162
 5.220D-04 1.500D 00 1.000D+00 5.000D+04 2.330D+04                          163
 ICONV=1                                                                    164
 5.000d-01 3.000d-01 2.000d-01 1.000d-01 8.000d-01 6.000d-01 3.000d-01      165
 2.000d-01 1.500d-01 1.000d-01 8.000d-01 6.000d-01 4.000d-01 2.500d-01      166
 .
 .
 .
 7.000d-01 5.500d-01 3.460d-01 3.000d-01 2.500d-01 2.150d-01 2.000d-01      172
 1.300d-01 1.000d-01 4.000d-01                                              173
 1.300d-01 1.000d-01 4.000d-01                                              174
```

C Output parameters and their meaning

C.1 Parameters and their meaning

Variable	Meaning	Line
RMAX	Outer cloud radius	6
RMIN	Inner cloud radius	7
RHOCS	Power law index (IDIST = 0) or $\frac{n_{\text{central}}}{n_{\text{surface}}}$ (IDIST = 1)	8
RHOBAR	Number density dust at center	9
TAU0F	Total optical depth to cloud center for IOF wavelength	11
NR	Number of grid points	12
NP	Number of impact parameters	13
NFD	Number of wavelength grid points	14
EPS	Maximum fractional error allowed for convergence	18
AJ0	Normalization constant for J*	19
ITMAX	Maximum number of iterations	20
IEDFTR	Use Eddington-Approximation: 0 = yes, 1 = no	25
IOUT	Output: 0 = 'normal' printout, 1 = detailed printout	26
IC	Central core: 0 = no, 1 = yes	27
NH	Use total net flux at core: 0 = no, 1 = yes	28
ISCA	Use first order scattering: 1 = yes, 0 = no	29
IB	Incident flux at outer boundary: 0 = yes, 1 = no	30
NMODEL	Number of models to run	31
AC(1)	Grain core radius in μ	37
AM(1)	Grain mantle radius in μ	38
TSTAR	Effective, specified Temperature central heat source for $\lambda > 912$ Å in Kelvin	50
TSTAR1	Effective Temperature of central heat source in Kelvin	51
RSTAR	Radius of central heat source in $R_\odot$	52
TLUM	Effective Luminosity central heat source for $\lambda > 912$ Å in $L_\odot$	53
TLUM1	Total Luminosity central heat source in $L_\odot$	54
SUMF	Integrated net flux for $\lambda > 912$ Åin ergs·sec^{-1}·Hz^{-1}·cm^{-2}	55
SUMF1	Total integrated net flux in ergs·sec^{-1}·Hz^{-1}·cm^{-2}	56
XRATIO	Fraction of energy for heating the grains in percent	57
IF	Reference wavelength index	58
MICRON	wavelength in μm	
QSCAI(NFD, N)	$Q_{\text{scattering}}\pi a^2$ at wavelength (in μm) for grain type N	
GBARI(NFD, N)	Scattering asymmetry parameter g for grain type ($0 \leq g \leq 1$)	
ALBEDI(NF, 5)	Albedo for each grain type at each wavelength	
IR	Reference radial grid index	119
R	Radial distance from center in $\frac{r}{R}$	
ABUNDI(N)	Fractional abundance of grain type N at each spatial grid point	
TDI(5, ND)	Temperature for each grain type	
FREQD(NF)	Wavelength in Hz	220
WFD(ND)	Quadrature weights for wavelength integration	
FLUXCD(NF)	Incident flux at inner boundary r_c $[H^+(R)]$	
FLUXSD(NFD)	Incident flux at outer boundary R $[H^-(R)]$	
TAUO	Total optical depth to cloud center at each wavelength	
RHOD(ND)	Dust number density ($n_d(r)$)	281
TD(ND)	Dust temperature ($T(r)$)	
TOF(ND)	Optical depth at each radius at reference wavelength IOF	
ITTERATION	Iteration number	281
ITCONT	Overall convergence: 0 = no, 1 = yes	
ITCONJ	Mean intensity convergence: 0 = no, 1 = yes	
DTD	Correction to dust temperature T	1812
DJD	Correction to mean intensity J	
...	Table continued at next page	...

Variable	Meaning	Line
DHD	Correction to Eddington flux $H(r)$	
FREQUENCY	Reference frequency index	1936
FREQ	Frequency in Hz	
LAMBDA	Wavelength in μ	
TF	$\frac{h\nu}{k}$	
FBD(NF)	Boundary factors at outer boundary $R(= f_B)$	
FCD(NF)	Boundary factors at inner boundary $r_c(f_C)$	
TB(ND)	Brightness temperature $T_{\rm B}$ from $J \equiv B(T_{\rm B})$	7853
TAU	Optical depth	
CHI(NF, ND)	Extinction coefficient $\chi(r)$ for isotropic scattering	
ETA(NF, ND)	Emissivity $\eta(r)$ for isotropic scattering	
FK(NF, ND)	Anisotropy factors $f(r)$	
ZETA(NF, ND)	Configuration function ζ	
AJ(NF, ND)	Mean intensity $J(r)$	
BJ	Planck function $B(T)$	
SOURCE(ND)	Source function ($\equiv \frac{\eta}{\chi}$)for at given frequency	
AH(NF, ND)	Eddington flux $H(r)$	
BDAHC(NF)	Net flux across inner boundary $H(r_c)$	7955
AHOUTC(NF)	Outward flux at inner core boundary r_c	
BDAHS(NF)	Net flux across outer boundary $H(R)$	
AHOUTS(NF)	Outward flux at boundary R	
OBS FLUX	Observed flux in ergs·sec^{-1}·sr^{-1}	
EIC(NF, 11)	Emergent flux at frequency and impact parameter	8016
IP	Impact parameter index	8078
XMU(NTHETA)	$\mu = \cos(\theta)$ in planar geometry (IGEOM = 0)	
THETA	Angle θ	
EMERG INT	Emerging intensity	9366
Y	Y location for convolved intensity from cloud center	9995
X	X location for convolved intensity from cloud center	9996
SIGMA(NF)	Half width of Gaussian beam pattern at each wavelength	
TAU0F	Total optical depth to cloud center for IOF wavelength	10615
AVFLUX(ND)	Frequency integrated net flux ($\equiv r^m H(r)$)	
COOLD(ND)	Total cooling rate in ergs·cm^{-3}·s^{-1}	
HEATD(ND)	Total heating rate in ergs·cm^{-3}·s^{-1}	
ABUNDI(5, ND)	Fractional abundance of each grain type at spatial grid point	10716
TDI(5, ND)	Temperature for grain type	
COOLDI(ND)	Cooling rate for grain type in ergs·cm^{-3}·sec^{-1}	
HEATDI(ND)	Heating rate for grain type in ergs·cm^{-3}·sec^{-1}	

Table 11: Output parameters and their meaning, for an example output file see Appendix C.2, line numbers refer to this file

C.2 Example output file

An example of an output file (the results from the test input file) is given below, see Table 11 in Appendix C.1 for the meaning of the parameters.

```
1                                        INPUT PARAMETERS FOR DUST CLOUD MODEL                                        1
                                                                                                                      2
                                                                                                                      3
                  MODEL PARAMETERS                                                                                    4
                                                                                                                      5
                                                  OUTER CLOUD RADIUS, RMAX = 5.220E-04 PARSECS                        6
                                                  INNER CLOUD RADIUS, RMIN =  7.830E-05 PARSECS                       7
                                    RATIO OF CENTRAL TO SURFACE DENSITIES, RHOCS =  1.000E+00                         8
                                        NUMBER DENSITY OF DUST AT CENTER, RHOBAR =  8.081E-03                         9
                                                                                                                      10
                                   TOTAL OPTICAL DEPTH ( 3.400E+00 MICRON), TAUOF =  1.500E+00                        11
                                                                                                                      12
                                                       NUMBER OF GRID POINTS, NR = 100                                13
                                                    NUMBER OF IMPACT PARAMETERS, NP = 109                             14
                                                    NUMBER OF FREQUENCY POINTS, NFD = 59                              15
                                                                                                                      16
                                                                                                                      17
                                                   CONVERGENCE PARAMETER, EPS =  1.000E-03                            18
                                                  NORMALIZATION CONSTANT, AJO =  1.000E-30                            19
                                                MAXIMUM NO. OF ITERATIONS, ITMAX =  20                                20
                                                                                                                      21
                                                                                                                      22
                                                                                                                      23
                                                                                                                      24
                                                EDDINGTON APPROXIMATION --- NO       (IEDFTR = 1)                     25
                                              DETAILED PRINTOUT OF RESULTS --- YES      (IOUT   = 1)                  26
                                                          CENTRAL CORE --- YES      (IC     = 1)                      27
                                         USE TOTAL NET FLUX AT INNER BOUNDARY --- YES      (NH     = 1)              28
                                           FIRST-ORDER ANISOTROPIC SCATTERING --- YES      (ISCA   = 1)              29
                                              INCIDENT FLUX AT OUTER BOUNDARY --- YES      (IB     = 1)              30
                                                          CLOUD GEOMETRY --- SPHERE   (IGEOM  = 2)                    31
                                                                                                                      32
                                                                                                                      33
                                                                                                                      34
                  DUST COMPONENT 1                                                                                    35
                                                                                                                      36
                                        RADIUS OF INNER CORE (CBOERSMA), AC =  5.000E-01 MICRON                       37
                                       RADIUS OF OUTER MANTLE (NOMANTLE), AM =  0.000E+00 MICRON                      38
                                                                                                                      39
                                                                                                                      40
                  DUST COMPONENT 2                                                                                    41
                                                                                                                      42
                                        RADIUS OF INNER CORE (silicate), AC =  5.000E-01 MICRON                       43
                                       RADIUS OF OUTER MANTLE (NOMANTLE), AM =  0.000E+00 MICRON                      44
                                                                                                                      45
                                                                                                                      46
                                                                                                                      47
                  CENTRAL HEAT SOURCE                                                                                 48
                                                                                                                      49
                                     SPECIFIED TEMPERATURE OF CENTRAL STAR, TSTAR =  5.000E+04 DEGREES                50
                                    EFFECTIVE TEMPERATURE OF CENTRAL STAR, TSTAR1 =  4.042E+04 DEGREES                51
                                                 RADIUS OF CENTRAL STAR, RSTAR =  3.141E+00 SOLAR RADII               52
                                       LUMINOSITY OF CENTRAL STAR .GE. 912A, TLUM =  2.330E+04 SOLAR UNITS            53
                                          TOTAL LUMINOSITY OF CENTRAL STAR, TLUM1 =  5.457E+04 SOLAR UNITS            54
                                              INTEGRATED NET FLUX .GE. 912A, SUMF =  1.204E+13 ERGS/(SEC*HZ*CM**2)    55
                                                TOTAL INTEGRATED NET FLUX, SUMF1 =  2.820E+13 ERGS/(SEC*HZ*CM**2)    56
                                 FRACTION OF ENERGY FOR HEATING THE GRAINS, XRATIO =  4.270E+01 PERCENT               57
1 IF     MICRON     QABSI( 1)   QSCAI( 1)   GBARI( 1)  ALBEDI( 1)   QABSI( 2)   QSCAI( 2)   GBARI( 2)  ALBEDI( 2)   58
                                                                                                                      59
   1    5.000E+03   1.070E-18   0.000E+00   0.000E+00   0.000E+00   1.070E-17   0.000E+00   0.000E+00   0.000E+00    60
    .
    .
    .
  59    9.100E-02   1.030E-11   0.000E+00   0.000E+00   0.000E+00   1.430E-11   9.150E-12   5.500E-02   3.902E-01    118

1 IR       R      ABUNDI( 1)  TDI( 1)   ABUNDI( 2)  TDI( 2)   ABUNDI(                                              119
9  1   1.500E-01  5.000E-01  1.500E+03  5.000E-01  1.500E+03                                                          120
.
.
.
9 100   1.000E+00  5.000E-01  8.260E+02  5.000E-01  8.260E+02                                                         219

1 IF    MICRON       FREQD       WFD        FLUXCD      FLUXSD       TAU0                                          220
                                                                                                                      221
   1  5.0000E+03  5.9958E+10  7.4948E+09  1.1303E-17  4.4275E-16  6.5112E-05                                         222
    .
    .
    .
  59  9.1000E-02  3.2944E+15  1.4825E+14  4.7699E-09  7.3750E-22  1.8670E+02                                         280
```

```
1 IR          R             RHOD           TD            TOF                                                                    281
9  1      1.500E-01      8.081E-03      1.500E+03      1.500E+00                                                               282
.
.
.
9 100      1.000E+00      8.081E-03      8.260E+02      0.000E+00                                                               381

1     ITERATION  1          ITCONT = 0          ITCONJ = 0                                                                    382
.
.
.
1     ITERATION 15          ITCONT = 1          ITCONJ = 1                                                                    1810
  IR          R             TD             DTD            DJD            DHD                                                  1811
9  1     1.5000E-01     2.9971E+03    -5.9828E-10    -8.5456E-06     0.0000E+00                                              1812
.
.
.
9 100     1.0000E+00     4.7673E+02    -9.7723E-06    -2.1087E-05     2.3129E-04                                              1911
1                                                                                                                            1912
.
.
.
                                        SUCCESSFUL CONVERGENCE AFTER 15 ITERATIONS                                           1932
                                                                                                                             1933
                                                                                                                             1934
                                     FINAL RESULTS FOR THERMAL PROPERTIES OF DIDC MODEL                                      1935
1**FREQUENCY  1**  FREQ = 5.996E+10 HERTZ  LAMBDA= 5.000E+03 MICRON  TF= 2.878E+00 DEGREE  FBD= 5.019E-01  FCD= 4.992E-01      1936
.
.
.
1**FREQUENCY 59**  FREQ = 3.294E+15 HERTZ  LAMBDA= 9.100E-02 MICRON  TF= 1.581E+05 DEGREE  FBD= 5.017E-01  FCD= 4.989E-01      7852
  IR      TB        TAU         TD        CHI        ETA         FK        ZETA         AJ         BJ       SOURCE       AH     7853
9  1  8.923E+03  1.867E+02  2.997E+03  1.364E-13  3.932E-22  3.304E-01  1.000E+00  1.064E-08  6.472E-24  2.884E-09  4.770E-09   7854
.
.
.
9 100  3.343E+03  0.000E+00  4.767E+02  1.364E-13  5.624E-35  3.349E-01  1.940E+01  1.521E-21  4.871-145  4.124E-22 -7.118E-22   7953

1                          PROPERTIES OF CONTINUUM RADIATION AT INNER AND OUTER BOUNDARIES                                    7954
  IF     FREQD     MICRON     BDAHC      FLUXCD     AHOUTC      FCD        BDAHS      FLUXSD     AHOUTS      FBD      OBS FLUX   7955
   1   5.996E+10  5.000E+03  1.130E-17  1.130E-17  0.000E+00  4.992E-01  1.179E-17  4.427E-16  4.545E-16  5.019E-01  5.712E-15   7956
   .
   .
   .
  59   3.294E+15  9.100E-02  4.770E-09  4.770E-09  0.000E+00  4.989E-01 -7.118E-22  7.375E-22  2.571E-23  5.017E-01  3.231E-22   8014

1                                        EMERGENT INTENSITIES AND FLUXES                                                     8015
 IF     MICRON     EIC(1)     EIC(3)     EIC(5)     EIC(7)     EIC(9)    EIC(10)    EIC(11)     FLUXCD     FLUXSD    OBS FLUX    8016
  1   5.000E+03  1.896E-15  1.899E-15  1.910E-15  1.920E-15  1.928E-15  1.934E-15  1.888E-15  1.420E-16  5.564E-15  5.712E-15    8017
  .
  .
  .
 59   9.100E-02  9.535E-23  9.554E-23  9.604E-23  9.620E-23  9.624E-23  9.625E-23  9.626E-23  5.994E-08  9.268E-21  3.231E-22    8075
1                            ANGULAR DISTRIBUTION OF EMERGENT INTENSITY FOR DUST COMPONENT                                    8076
                                                                                                                             8077
     IP =   1    TAU =  1.500E+00     XMU =  1.000E+00     THETA =  0.000E+00                                                 8078
     .
     .
     .
     IP = 100    TAU =  1.765E-03     XMU =  4.471E-02     THETA =  8.744E+01                                                 9365
 EMERG INT  1.773E-15 ( 2.802E+00)  5.998E-16 ( 1.481E+00)  3.259E-15 ( 2.809E+00)  4.247E-15 ( 2.831E+00)  4.848E-15 ( 3.257E+00)  9366
 .
 .
 .
 EMERG INT -2.628E-21 ( 0.000E+00) -2.928E-21 ( 0.000E+00) -1.796E-21 ( 0.000E+00) -1.286E-21 ( 0.000E+00)                    9377

1                              ANGULAR DISTRIBUTION OF EMERGENT INTENSITY AT SELECTED WAVELENGTHS                             9378
   I       R      ( 5.00E+03)( 4.00E+03)( 3.00E+03)( 2.00E+03)( 1.00E+03)( 8.00E+02)( 6.00E+02)( 4.50E+02)( 4.00E+02)( 3.00E+02)  9379
.
.
.
1                              ANGULAR DISTRIBUTION OF EMERGENT INTENSITY AT SELECTED WAVELENGTHS                             9893
   I       R      ( 2.15E-01)( 2.10E-01)( 2.00E-01)( 1.80E-01)( 1.43E-01)( 1.30E-01)( 1.10E-01)( 1.00E-01)( 9.10E-02)(        9894
9  1   1.500E-01  9.712E-22  9.290E-22  9.649E-22  8.080E-22  3.171E-22  2.522E-22  3.051E-23  1.575E-22  9.535E-23             9895
.
.
.
9 100   1.000E+00 -1.734E-21 -1.599E-21 -1.158E-21 -1.086E-21 -2.376E-21 -2.628E-21 -2.928E-21 -1.796E-21 -1.286E-21             9994

1                          CONVOLVED INTENSITIES, AT GIVEN X AND Y  FROM CLOUD CENTER Y = 0.000                               9995
9 IF    MICRON   SIGMA   X = 0.0   X=0.111   X=0.222   X=0.333   X=0.444   X=0.556   X=0.667   X=0.778   X=0.889   X=1.000     9996
.
.
.
9  1 5.000E+03 5.000E-01 1.589E-15 1.574E-15 1.539E-15 1.473E-15 1.399E-15 1.282E-15 1.159E-15 1.031E-15 8.701E-16 7.219E-16   9998

1                          CONVOLVED INTENSITIES, AT GIVEN X AND Y  FROM CLOUD CENTER Y = 1.000                               10553
9 IF    MICRON   SIGMA   X = 0.0   X=0.111   X=0.222   X=0.333   X=0.444   X=0.556   X=0.667   X=0.778   X=0.889   X=1.000     10554
```

```
                                                                                                                                      10555
9  1 5.000E+03 5.000E-01 7.219E-16 7.132E-16 6.952E-16 6.551E-16 6.208E-16 5.220E-16 4.923E-16 3.893E-16 3.400E-16 2.777E-16            10556
.
.
.
9 59 9.100E-02 4.000E-01 5.049E-23 4.905E-23 4.905E-23 4.110E-23 4.228E-23 3.356E-23 3.147E-23 2.163E-23 1.954E-23 1.223E-23            10614

1 IR       R         RHOD       TAUOF       TD        AVFLUX      COOLD      HEATD                                                        10615
9  1   1.500E-01  8.081E-03  1.500E+00  2.997E+03  5.754E+35  1.637E-05  1.637E-05                                                       10616
.
.
.
9 100   1.000E+00  8.081E-03  0.000E+00  4.767E+02  5.755E+35  3.276E-09  3.276E-09                                                      10715

1 IR      R      ABUNDI( 1)  TDI( 1)   COOLDI( 1) HEATDI( 1) ABUNDI( 2)  TDI( 2)   COOLDI( 2) HEATDI( 2)                                  10716
9  1   1.500E-01  5.000E-01  1.996E+03  8.240E-06  8.240E-06  5.000E-01  3.422E+03  8.134E-06  8.134E-06                                 10717
.
.
.
9 100   1.000E+00  5.000E-01  4.334E+02  1.635E-09  1.635E-09  5.000E-01  2.868E+02  1.641E-09  1.641E-09                                10816
```

D Generated input file to run with CSDUST3

```
NMODEL=  1
 IGEOM=2 IEMRG=1
IEDFTR=0  IOUT=1    IC=1    NH=1  ISCA=1    IB=1 IDIST=0
 1.000D-30  1.000D-03 35
 2.229d-01 2.230d-01 2.231d-01 2.234d-01 2.238d-01 2.244d-01 2.251d-01
 2.259d-01 2.268d-01 2.280d-01 2.292d-01 2.306d-01 2.321d-01 2.338d-01
 2.357d-01 2.377d-01 2.398d-01 2.421d-01 2.446d-01 2.472d-01 2.499d-01
 2.528d-01 2.559d-01 2.591d-01 2.625d-01 2.661d-01 2.698d-01 2.737d-01
 2.777d-01 2.819d-01 2.862d-01 2.907d-01 2.954d-01 3.003d-01 3.053d-01
 3.104d-01 3.158d-01 3.213d-01 3.269d-01 3.328d-01 3.388d-01 3.449d-01
 3.513d-01 3.578d-01 3.644d-01 3.713d-01 3.783d-01 3.855d-01 3.928d-01
 4.003d-01 4.080d-01 4.159d-01 4.239d-01 4.321d-01 4.405d-01 4.491d-01
 4.578d-01 4.667d-01 4.757d-01 4.850d-01 4.944d-01 5.040d-01 5.137d-01
 5.237d-01 5.338d-01 5.441d-01 5.546d-01 5.652d-01 5.760d-01 5.870d-01
 5.982d-01 6.095d-01 6.210d-01 6.327d-01 6.446d-01 6.567d-01 6.689d-01
 6.813d-01 6.939d-01 7.067d-01 7.196d-01 7.328d-01 7.461d-01 7.596d-01
 7.732d-01 7.871d-01 8.011d-01 8.153d-01 8.297d-01 8.443d-01 8.590d-01
 8.740d-01 8.891d-01 9.044d-01 9.199d-01 9.355d-01 9.514d-01 9.674d-01
 9.836d-01 1.000d+00
   60   20
 2.000d 03 1.300d 03 1.100d 03 1.099d 03 8.001d 02 8.000d 02 7.999d 02
 7.998d 02 4.500d 02 4.499d 02 4.000d 02 3.999d 02 3.500d 02 3.000d 02
 2.350d 02 2.000d 02 1.600d 02 1.200d 02 1.000d 02 9.500d 01 9.499d 01
 9.000d 01 8.000d 01 7.000d 01 6.000d 01 5.000d 01 4.700d 01 4.000d 01
 3.300d 01 3.000d 01 2.500d 01 2.000d 01 1.999d 01 1.800d 01 1.300d 01
 1.100d 01 1.000d 01 9.999d 00 8.000d 00 6.000d 00 4.800d 00 4.000d 00
 3.500d 00 3.000d 00 2.200d 00 1.800d 00 9.000d-01 7.000d-01 5.500d-01
 4.350d-01 3.460d-01 2.750d-01 2.500d-01 2.150d-01 2.000d-01 1.800d-01
 1.430d-01 1.300d-01 1.000d-01 9.100d-02
 4.119d-15 2.904d-15 2.535d-15 2.533d-15 1.264d-15 1.264d-15 1.263d-15
 1.262d-15 1.459d-17 1.457d-17 7.064d-18 7.070d-18 1.065d-17 1.712d-17
 6.290d-18 2.975d-17 2.334d-17 1.035d-17 4.192d-17 2.058d-17 2.055d-17
 9.723d-18 8.912d-18 7.732d-18 5.674d-18 3.947d-18 3.086d-18 1.624d-18
 7.459d-19 5.073d-19 2.368d-19 9.350d-20 9.352d-20 9.850d-20 1.040d-19
 1.068d-19 1.080d-19 1.079d-19 8.025d-20 1.100d-19 1.546d-19 2.010d-19
 2.392d-19 2.874d-19 3.860d-19 4.363d-19 3.544d-20 2.479d-20 1.577d-20
 9.424d-20 5.150d-20 2.295d-20 1.504d-20 1.422d-20 1.374d-20 1.333d-20
 1.229d-20 1.143d-20 4.849d-21 2.949d-21
    1
DRAINELI  5.000D-01 NOMANTLE  0.000D 00  1
 2.176d-27 0.000d 00-2.558d-03 2.000d 03
 4.483d-27 0.000d 00-3.800d-03 1.300d 03
 5.932d-27 0.000d 00-4.200d-03 1.100d 03
 5.941d-27 0.000d 00-4.200d-03 1.099d 03
 1.013d-26 0.000d 00-4.800d-03 8.001d 02
 1.014d-26 0.000d 00-4.800d-03 8.000d 02
 1.014d-26 0.000d 00-4.800d-03 7.999d 02
 1.014d-26 0.000d 00-4.800d-03 7.998d 02
 2.842d-26 0.000d 00-5.300d-03 4.500d 02
 2.844d-26 0.000d 00-5.300d-03 4.499d 02
 3.582d-26 0.000d 00-5.200d-03 4.000d 02
 3.584d-26 0.000d 00-5.200d-03 3.999d 02
 4.703d-26 0.000d 00-5.162d-03 3.500d 02
 6.522d-26 0.000d 00-4.900d-03 3.000d 02
 1.110d-25 0.000d 00-4.343d-03 2.350d 02
 1.541d-25 0.000d 00-3.700d-03 2.000d 02
 2.450d-25 0.000d 00-2.067d-03 1.600d 02
 4.416d-25 0.000d 00 2.529d-03 1.200d 02
 6.425d-25 0.000d 00 7.100d-03 1.000d 02
 7.164d-25 0.000d 00 8.091d-03 9.500d 01
 7.166d-25 0.000d 00 8.093d-03 9.499d 01
 8.040d-25 0.000d 00 9.031d-03 9.000d 01
 1.036d-24 0.000d 00 9.900d-03 8.000d 01
 1.382d-24 0.000d 00 7.210d-03 7.000d 01
 1.919d-24 1.919d-28-1.229d-04 6.000d 01
 2.786d-24 2.786d-28-1.142d-02 5.000d 01
 3.141d-24 3.141d-28-1.443d-02 4.700d 01
 4.244d-24 4.244d-28-1.912d-02 4.000d 01
 5.834d-24 1.167d-27-2.286d-02 3.300d 01
 6.830d-24 1.366d-27-2.390d-02 3.000d 01
 9.322d-24 2.797d-27-2.412d-02 2.500d 01
 1.435d-23 7.177d-27-2.384d-02 2.000d 01
 1.437d-23 7.185d-27-2.383d-02 1.999d 01
 1.617d-23 1.116d-26-2.509d-02 1.800d 01
 1.341d-23 4.023d-26-2.870d-02 1.300d 01
 2.831d-23 8.209d-26-3.094d-02 1.100d 01
 4.073d-23 1.222d-25-3.440d-02 1.000d 01
 4.074d-23 1.222d-25-3.440d-02 9.999d 00
 1.528d-23 2.477d-25-5.035d-02 8.000d 00
 9.341d-24 8.022d-25-5.283d-02 6.000d 00
 1.185d-23 1.874d-24-4.245d-02 4.800d 00
 1.582d-23 3.530d-24-2.194d-02 4.000d 00
 1.967d-23 5.376d-24 1.895d-03 3.500d 00
 2.528d-23 8.355d-24 3.937d-02 3.000d 00
 4.133d-23 1.792d-23 1.293d-01 2.200d 00
 5.588d-23 2.737d-23 1.837d-01 1.800d 00
 1.516d-22 9.572d-23 3.980d-01 9.000d-01
 2.173d-22 1.435d-22 4.782d-01 7.000d-01
 3.053d-22 2.029d-22 5.403d-01 5.500d-01
 4.173d-22 2.688d-22 5.734d-01 4.350d-01
```

```
5.458d-22 3.307d-22 5.780d-01 3.460d-01
6.946d-22 3.922d-22 5.575d-01 2.750d-01
8.196d-22 4.306d-22 5.506d-01 2.500d-01
1.171d-21 4.920d-22 5.624d-01 2.150d-01
1.026d-21 4.607d-22 5.832d-01 2.000d-01
9.017d-22 4.087d-22 6.204d-01 1.800d-01
1.059d-21 3.833d-22 6.772d-01 1.430d-01
1.182d-21 4.054d-22 6.824d-01 1.300d-01
1.796d-21 4.851d-22 6.518d-01 1.000d-01
2.024d-21 4.943d-22 6.644d-01 9.100d-02
1.000D 00
   0      1.000D 01 1.000D 03
0.350D 00 0.300D 00 9.999D-01 2.500D+04 2.500D+05
ICONV=1
3.680d-01 2.638d-01 2.571d-01 2.503d-01 2.571d-01 2.165d-01 1.894d-01
1.894d-01 2.368d-01 1.894d-01 6.629d-01 4.735d-01 2.029d-01 1.353d-04
1.353d-04 1.353d-04 1.353d-04 1.353d-04 4.059d-01 4.059d-01 3.788d-01
1.353d-04 1.353d-04 1.353d-04 1.353d-04 4.059d-01 2.976d-01 1.353d-04
1.826d-01 4.059d-01 1.826d-01 1.826d-01 1.353d-01 1.353d-04 1.015d-01
1.353d-04 1.015d-01 1.353d-01 1.015d-01 1.353d-04 1.353d-01 1.353d-04
1.353d-01 1.353d-04 1.353d-01 1.353d-04 1.353d-04 1.353d-04 1.353d-04
1.353d-04 1.353d-04 1.353d-04 1.353d-04 1.353d-04 1.353d-04 1.353d-04
1.353d-04 1.353d-04 1.353d-04 1.353d-04
```

E Tabulated results for the density and temperature profiles

$\frac{r}{R}$	Dust number density	Temperature (K)
2.229e-01	6.058e+00	1.754e+02
2.230e-01	6.058e+00	1.666e+02
2.231e-01	6.058e+00	1.584e+02
2.234e-01	6.058e+00	1.389e+02
2.238e-01	6.058e+00	1.195e+02
2.244e-01	6.058e+00	1.016e+02
2.251e-01	6.058e+00	9.036e+01
2.259e-01	6.058e+00	8.446e+01
2.268e-01	6.057e+00	8.153e+01
2.280e-01	6.054e+00	7.975e+01
2.292e-01	6.052e+00	7.869e+01
2.306e-01	6.049e+00	7.780e+01
2.321e-01	6.046e+00	7.702e+01
2.338e-01	6.043e+00	7.624e+01
2.357e-01	6.040e+00	7.544e+01
2.377e-01	6.036e+00	7.466e+01
2.398e-01	6.032e+00	7.388e+01
2.421e-01	6.028e+00	7.307e+01
2.446e-01	6.024e+00	7.224e+01
2.472e-01	6.019e+00	7.142e+01
2.499e-01	6.015e+00	7.061e+01
2.528e-01	6.009e+00	6.978e+01
2.559e-01	6.004e+00	6.894e+01
2.591e-01	5.999e+00	6.812e+01
2.625e-01	5.993e+00	6.729e+01
2.661e-01	5.987e+00	6.645e+01
2.698e-01	5.981e+00	6.563e+01
2.737e-01	5.975e+00	6.481e+01
2.777e-01	5.969e+00	6.401e+01
2.819e-01	5.962e+00	6.321e+01
2.862e-01	5.955e+00	6.243e+01
2.907e-01	5.949e+00	6.165e+01
2.954e-01	5.942e+00	6.088e+01
3.003e-01	5.935e+00	6.011e+01
3.053e-01	5.927e+00	5.937e+01
3.104e-01	5.920e+00	5.864e+01
3.158e-01	5.913e+00	5.791e+01
3.213e-01	5.905e+00	5.720e+01
3.269e-01	5.898e+00	5.652e+01
3.328e-01	5.890e+00	5.582e+01
3.388e-01	5.882e+00	5.515e+01
3.449e-01	5.874e+00	5.451e+01
3.513e-01	5.866e+00	5.386e+01
3.578e-01	5.859e+00	5.323e+01
3.644e-01	5.851e+00	5.262e+01
3.713e-01	5.842e+00	5.201e+01
3.783e-01	5.834e+00	5.143e+01
3.855e-01	5.826e+00	5.085e+01
3.928e-01	5.818e+00	5.029e+01
4.003e-01	5.810e+00	4.974e+01
4.080e-01	5.802e+00	4.921e+01
4.159e-01	5.793e+00	4.868e+01
4.239e-01	5.785e+00	4.817e+01
4.321e-01	5.777e+00	4.767e+01
4.405e-01	5.768e+00	4.718e+01
4.491e-01	5.760e+00	4.671e+01
4.578e-01	5.752e+00	4.624e+01
4.667e-01	5.743e+00	4.579e+01
4.757e-01	5.735e+00	4.535e+01
4.850e-01	5.726e+00	4.492e+01
4.944e-01	5.718e+00	4.450e+01
5.040e-01	5.710e+00	4.409e+01
5.137e-01	5.701e+00	4.370e+01
5.237e-01	5.693e+00	4.331e+01
5.338e-01	5.685e+00	4.293e+01
5.441e-01	5.677e+00	4.256e+01
5.546e-01	5.668e+00	4.220e+01
5.652e-01	5.660e+00	4.185e+01
5.760e-01	5.652e+00	4.151e+01
5.870e-01	5.644e+00	4.118e+01
5.982e-01	5.635e+00	4.086e+01
6.095e-01	5.627e+00	4.055e+01
6.210e-01	5.619e+00	4.024e+01
6.327e-01	5.611e+00	3.995e+01
6.446e-01	5.603e+00	3.966e+01
6.567e-01	5.595e+00	3.938e+01
6.689e-01	5.587e+00	3.911e+01
6.813e-01	5.579e+00	3.885e+01
6.939e-01	5.571e+00	3.859e+01
7.067e-01	5.563e+00	3.835e+01

Continued ⇓ *Continued* ⇓ *Continued* ⇓

$\frac{r}{R}$	Dust number density	Temperature (K)
7.196e-01	5.555e+00	3.811e+01
7.328e-01	5.547e+00	3.788e+01
7.461e-01	5.539e+00	3.765e+01
7.596e-01	5.532e+00	3.744e+01
7.732e-01	5.524e+00	3.723e+01
7.871e-01	5.516e+00	3.702e+01
8.011e-01	5.509e+00	3.683e+01
8.153e-01	5.501e+00	3.664e+01
8.297e-01	5.493e+00	3.646e+01
8.443e-01	5.486e+00	3.628e+01
8.590e-01	5.478e+00	3.611e+01
8.740e-01	5.471e+00	3.595e+01
8.891e-01	5.463e+00	3.579e+01
9.044e-01	5.456e+00	3.564e+01
9.199e-01	5.448e+00	3.550e+01
9.355e-01	5.441e+00	3.536e+01
9.514e-01	5.434e+00	3.522e+01
9.674e-01	5.427e+00	3.509e+01
9.836e-01	5.419e+00	3.497e+01
1.000e+00	5.412e+00	3.486e+01

Table 12: Tabulated results CSDUST3 on Density and Temperature profile.